



# The Six Dwarfs of the Middle East: revision of the enigmatic praying mantis genus *Holaptilon* (Mantodea: Gonypetidae: Gonypetinae) with the description of four new species under integrative taxonomy

Zohreh Mirzaee<sup>1,2,3</sup>, Roberto Battiston<sup>4</sup>, Francesco Ballarin<sup>5</sup>, Saber Sadeghi<sup>3</sup>, Marianna Simões<sup>1,6</sup>, Martin Wiemers<sup>1</sup>, Thomas Schmitt<sup>1,2</sup>

1 Senckenberg German Entomological Institute, Eberswalder Str. 90, 15374 Müncheberg, Germany

2 Entomology and Biogeography, Institute of Biochemistry and Biology, Faculty of Science, University of Potsdam, 14476 Potsdam, Germany

3 Biology Department, Faculty of Sciences, Shiraz University, Shiraz, Iran

4 Museo di Archeologia e Scienze Naturali “G. Zannato”, Montecchio Maggiore, Italy

5 Systematic Zoology Laboratory, Department of Biological Sciences, Tokyo Metropolitan University, 1-1 Minami-Osawa, Hachioji-shi, 192-0397, Tokyo, Japan

6 Senckenberg Research Institute and Natural History Museum, Senckenberganlage 25, 60325 Frankfurt am Main, Germany

<https://zoobank.org/DCA8C2DB-979F-42B1-9C8D-99FAA60BFE80>

Corresponding author: Zohreh Mirzaee (zmirzaee1988@gmail.com)

Received 16 September 2023

Accepted 5 December 2023

Published 18 March 2024

Academic Editors Monika Eberhard, Klaus-Dieter Klass

**Citation:** Mirzaee Z, Battiston R, Ballarin F, Sadeghi S, Simões M, Wiemers M, Schmitt T (2024) The Six Dwarfs of the Middle East: revision of the enigmatic praying mantis genus *Holaptilon* (Mantodea: Gonypetidae: Gonypetinae) with the description of four new species under integrative taxonomy. *Arthropod Systematics & Phylogeny* 82: 89–117. <https://doi.org/10.3897/asp.82.e112834>

## Abstract

The dwarf-mantid genus *Holaptilon* Beier, 1964 is composed of small-sized ground-runner species distributed in the Middle East. Due to their elusive lifestyle, little is known about their behaviour, distribution, and phylogeny. The genus *Holaptilon* was once established for a single species, *H. pusillum* Beier, 1964, based on material collected in Jerusalem, Israel. Later, *H. brevipugilis* Kolnegari, 2018, and *H. yagmur* Yılmaz and Sevgili, 2023 were described from Iran and Turkey, respectively. In this study, integrated morphology, molecular analyses, and ecology were used to revise the genus *Holaptilon* and define the boundaries of its species. New data on this genus are presented, based on *Holaptilon* specimens collected from various provinces of Iran, Israel, Jordan, and Turkey. Extensive analyses, including examinations of male and female genitalia, morphometrical analysis, and morphological hypervolumes were conducted to distinguish its species morphologically. In addition, four molecular markers (mitochondrial and nuclear) were studied to gain a better understanding of species delimitation and phylogenetic relationships. As a result, impressive inter- and intraspecific variability was recovered. In addition to the three already known species, four new species with their distributions restricted to Iran (*H. abduallahii* sp. nov., *H. khozestani* sp. nov., *H. iranicum* sp. nov., and *H. tadovaniensis* sp. nov.) are here described, and *H. yagmur* Yılmaz and Sevgili, 2023 is synonymized with *H. brevipugilis* Kolnegari, 2018. The integrative approach was essential for an adequate classification in *Holaptilon* taxonomy and also helpful in the clarification of problematic and cryptic Mantodea species. Additional information concerning the life cycle, ecological aspects, spermatophore feeding, as well as geographical range and historical biogeography of *Holaptilon* species is also provided.

## Keywords

Autecology, biogeography, morphology, species delimitation, species descriptions, systematics

## 1. Introduction

The genus *Holaptilon* Beier, 1964 (Gonypetidae, Gonypetinae) was established from a single species, *Holaptilon pusillulum* Beier, 1964, on the basis of three specimens (two males, one female) sampled in Jerusalem, Israel. After the original description, no further records were published for the next 43 years until Abu-Dannoun and Katbeh-Bader (2007) reported three additional specimens from Jordan. Ten years later, Handal et al. (2018) recorded a single female, confirming the presence of this species at its type locality. The same year, *Holaptilon brevipugilis* Kolnegari, 2018, was described from Iran. Recently, another species, *Holaptilon yagmur* Yılmaz and Sevgili, 2023, was described from Turkey. Both new species were described based on a few qualitative characters (except for the number of tibial spines in *H. yagmur*), not assessing intraspecific variability. The systematic placement of the genus *Holaptilon* was recently changed from the family Mantidae to Gonypetidae; its subfamily changed from Amelinae to Gonypetinae (Schwarz and Roy 2019) but till now no molecular data or knowledge regarding male genitalia of *Holaptilon* was available to support this assessment. In addition, the species composition in this genus and their taxonomic status remained enigmatic, because all species descriptions were based on rather limited numbers of specimens and relied on subtle and often questionable morphological characters. This made their systematic assessments rather vague. However, advanced tools in integrative taxonomy now allow for more sophisticated analyses, more successfully addressing such problems. For example, morphological hypervolume analyses are used to compare the morphological characteristics of different species, and the degree of overlap between hypervolumes can provide insight into the degree of morphological similarity or difference between species. By using hypervolume analyses, patterns of variation not being apparent using traditional taxonomic methods can be better addressed. This is particularly useful in cases where species or populations are difficult to distinguish based on morphological characters alone. This approach can also provide a more quantitative and objective way of comparing morphological data than traditional taxonomic methods, which can frequently be influenced by subjective interpretation. Overall, using hypervolume analyses for morphological data is a promising approach for addressing taxonomic problems, and can lead to more accurate and robust taxonomic classifications (Blonder et al. 2014).

Species delimitation analyses using molecular data also play a crucial role in resolving taxonomic uncertainties and distinguishing putative species with unclear morphology (Vitecek et al. 2017). In this study, species delimitation analyses based on molecular data were used as a crucial tool to address taxonomic challenges within the genus. By incorporating them, we tried to resolve ambiguous species boundaries in the genus *Holaptilon* and to identify putative species with unclear morphol-

ogy. This approach played a significant role in enhancing our understanding of this genus and allowed us to overcome taxonomic problems, ultimately contributing to a more comprehensive and accurate assessment of its diversity. In this study, the species boundaries of *Holaptilon* were tested, evaluating the intra- and inter-specific variability and defining the diversity within the genus using an integrative approach, combining different morphological analyses with a multigene molecular analysis. New specimens were collected during extensive field surveys in Iran, and the examination of these samples suggested the presence of new putative species previously unknown to science. The results of this study also contribute to the understanding of the biogeography and conservation of this rare genus, preliminarily assessing its conservation status, species diversity, endemism, and peculiar ecology.

## 2. Material and methods

### 2.1. Distribution records, field collection, laboratory rearing, and deposition of specimens

Occurrence records of *Holaptilon* were harvested from previous studies (Abu-Dannoun and Katbeh-Bader 2007: one record; Kolnegari and Vafaei 2018: three records; Handal et al. 2018: one record; Yılmaz and Sevgili 2023: three records) and complemented with freshly collected samples (79 records) from Iran, old collected samples (four records) plus freshly collected samples (two records) from Israel, and records extracted from the iNaturalist portal (these records were checked carefully for correct identification and curated by the first author), i.e. five records with IDs: 179338809, 147924203, 147924202, 147924201, 147924199, 81544213). A total of 87 records was obtained and plotted on a distribution map using QGIS v. 3.22. The complete list of records is reported in Table S1.

Fresh specimens and oothecae were collected over a seven-year period (2015–2021) from 15 districts in six provinces of Iran (Mashhad, Khorasan Razavi Province; Arak, Markazi Province; Yasuj, Kohgiluyeh va Buier Ahmad Province; Dehdez, Mal agha, Bagh Malek, and Gharibiha village, Khozestan Province; Dasht Arjan, Fasa, Tadovan, and Sahlak, Fars Province; Sooro, Kangan, Tombak, and Jam, Bushehr Province). Sampling methods included net sweeping and hand-picking during daytime through careful observation under stones or observing mantids running on the surface of stones, and at night-time mostly on the ground or attracted to some source of light. Once collected, specimens were put in separate plastic containers and later placed in separate plastic jars (15 × 15 × 10 cm) after arriving at the laboratory. Some rocks and sticks were added to the container in order to help the mantids climb and hang, especially during moulting.

The specimens of the four species newly described in this study are deposited in the following institutions or private collections: **ESPC** Evgeny Shcherbakov, Private Collection, Ramenskoye, Russia; **ZMCBSU** The Zoology Museum of Shiraz University, Shiraz, Iran; **ZMPC** Zohreh Mirzaee, Private Collection, Müncheberg, Germany; **SDEI** Senckenberg German Entomological Institute, Müncheberg, Germany. Other examined material is deposited in the following institutions or private collections: **HSC** Hasan Sevgili collection (Department of Molecular Biology and Genetic, Ordu University, Turkey); **SMNHTAU** The Steinhardt Museum of Natural History, Tel Aviv, Israel.

## 2.2. Living specimen observations

Specimens in the lab were observed throughout their entire lifetime. At adult stage, males and females were placed together to observe their mating behaviour. Once laid, the oothecae were collected to record the following data: number of hatching nymphs, number of instars to reach adult stage, male and female rate per ootheca, male and female longevity, and spermatophore feeding. Information from the oothecae oviposited in the lab was compared with oothecae oviposited in their natural habitat. The individuals were kept at room temperature (25–27°C), with relative air humidity (RH) kept at 50–55% by misting the room on a regular basis. An HTC2 digital terrarium hygrometer (Dongguan, China) was used to monitor RH. According to some occasional observations of the specimens preying on small ants and small flies in nature, laboratory specimens were fed with one to two fruit flies (*Drosophila melanogaster* Meigen, 1830) or small ants (*Trichomyrmex* spec.) every third day. Later instars were fed with living mealworm larvae (*Tenebrio molitor* Linnaeus, 1758) twice a week, all after testing the appreciation and response of this mantid toward these unconventional preys.

## 2.3. Dissections

After completing their life cycle, the individuals were preserved in 96% ethanol for morphological and molecular studies. Specimens were examined and measurements were taken under a Leica M205 C stereomicroscope with an ocular micrometer. The classification system used in this study follows Schwarz and Roy (2019). Descriptive terminology of external morphology of male, female and preparation of male genitalia followed Brannoch et al. (2017). The ultimate segments of male abdomina were dissected under a stereomicroscope, in order to separate the genitalia from the terminalia. Genitalia were macerated as a whole in 10% KOH solution. Subsequently, they were washed first with distillate water, then in ethanol (70%), and finally in glycerine for 24 hours in order to ensure the complete removal of ethanol. Finally, prepared genitalia were placed in a vial with glycerine drops for further study. The specimens were photographed with a

system comprising a Stone Master Stack Unit, an Olympus OM-D E-M1 Mark II camera, and Zeiss Luminar lenses (16 mm, 25 mm, 40 mm, 63 mm). Olympus Capture and Stone Master v.3.8 software was used to acquire digital photos. Stacking was performed with Helicon Focus (v.7.6.1), and a scalebar was added with ImageJ (v.1.53t).

## 2.4. Morphometric analyses, measurements and morphological hypervolume calculations

Most of the traditional taxonomy in Mantodea, especially at the genus/species level, is based on external morphological characters, and all current species delimitation in the genus *Holaptilon* is based on few qualitative characters like the shape of the pronotum and the tip of the supra-anal plate (= 10<sup>th</sup> abdominal tergite), the pattern of the fore femora inner colour spot, and the number of posteroventral tibial spines (Yılmaz and Sevgili 2023). Considering the type specimens of all three already known *Holaptilon* species, the current taxonomy is based on just ten specimens, a clearly insufficient number to measure inter- and intraspecific variability within this genus. To evaluate this variability, all of these characters were considered and studied in a larger number of specimens. Moreover, all the further traditional measures and ratios used as discriminants in Mantodea, including shapes of male and female genitalia, were also included in our analyses.

To measure morphological differentiation among *Holaptilon* species, volumes and overlaps of morphological traits and their respective centroid distances were calculated using the R package Hypervolume (Blonder et al. 2014). Three sets of measurements, including spine counting on both left and right front legs (AFS, PFS, ATS, PTS, DS), ratios of different body parts in relation to each other, and measurements of different parts of the body (Tables S2–S4) were used. In total, 16 measurements (see below) for all *Holaptilon* specimens were considered in this study. All spines from both the right and left frontal legs (see below) of each specimen were counted and the distances between different body parts measured and then the ratios were calculated.

### Measurement classes:

- 1 Total body length (TBL) = body length measured from the most anterior margin of the head to the posterior tip of styli in male and tips of gonopods in female (Brannoch et al. 2017: fig. 25D).
- 2 Pronotum length (PL) = distance from the anterior to the posterior margin of the pronotum at midline.
- 3 Pronotum width (PW) = distance between the lateral margins of the pronotum at the widest point.
- 4 Mesonotum length (Mes L) = distance from the anterior to the posterior margin of the mesonotum at midline.
- 5 Mesonotum width (Mes W) = distance between the lateral margins of the mesonotum at the widest point.

- 6 Metanotum length (Met L) = distance from the anterior to the posterior margin of the metanotum at midline.
- 7 Metanotum width (Met W) = distance between the lateral margins of the metanotum at the widest point.
- 8 Head height (HH) = distance between the tip of the labrum and the top of the vertex at midline (Brannoch et al. 2017: fig. 24B, but height of labrum additionally included).
- 9 Head width (HW) = distance between the lateral margins of the eyes at the widest point (Brannoch et al. 2017: fig. 24A).
- 10 Lower frons height (LFH) = distance between the antennal insertions to the upper margin of the clypeus at midline (Brannoch et al. 2017: fig. 24D).
- 11 Lower frons width (LFW) = greatest distance between the mediolateral margin of the lower frons to the opposing margin (Brannoch et al. 2017: fig. 24C).
- 12 Prothoracic coxae length (P Coxa) = distance from proximal margin abutting pronotum to trochanter (on ventral side).
- 13 Prothoracic femora length (P Fem L) = distance from proximal margin abutting trochanter to distal margin of genicular lobe (on ventral side).
- 14 Prothoracic femora width (P Fem W) = width of the femora at the widest point.
- 15 Prothoracic tibiae length (P Tibia L) = distance from distal margin of genicular lobe to the tip of distal terminal spur.
- 16 Prothoracic tarsus length (P Tarsus L) = distance from the tarsal insertion point on the tibia to the distal terminus of the 5th tarsomere (on ventral side).

### Spine counts on foreleg:

- 1 Anteroventral femoral spine count (AFS) = number of all inner marginal ridge spines but excluding the genicular spine.
- 2 Posteroventral femoral spine count (PFS) = number of all outer marginal ridge spines but excluding the genicular spine.
- 3 Anteroventral tibial spine count (ATS) = number of all inner marginal ridge spines but excluding the distal terminal spur.
- 4 Posteroventral tibial spine count (PTS) = number of all outer marginal ridge spines but excluding the distal terminal spur.
- 5 Discoidal spines (DS) = number of discoidal spines.

We used a multimodal approach to evaluate the existence of different morphospecies within the genus *Holaptilon* and to trace morphological boundaries between them, using traditional morphology to support or reject the molecular phylogeny. First, all the mean values of the more traditional discriminative morphological ratios (as in: Obertegger and Agabiti 2012) for Mantodea (PL/PW, HH/HW, LFW/LFH, FL/FW, MsL/MsW, MtL/MtW, HW/PW, PL/HH; meanings of abbreviations are given below in measurement classes section) were compared in both males and females to identify the two most discrim-

inative ones. Then, the single values of these two ratios were plotted to visualise the distinctiveness of putative species in the morpho-space. As a third step, all ratios were plotted with the Bioinformatics online platform for data analysis and visualisation (<http://www.bioinformatics.com.cn/srplot>) as a dendrogram using a simple Euclidean algorithm with complete distances.

Species-scale hypervolumes with (i) measurements axes, (ii) ratio axes, and (iii) a number of spine axes were defined. Hypervolumes can only be estimated when the number of observations (m) and dimensionality (n) are greater than two. Therefore, species known from only one (i.e., the holotype) or with no specimens available (i.e., lost) should be excluded from morphological analyses. The same applies to the number of axes, as hypervolumes can only be compared if they are constructed using the same axes (Blonder et al. 2014); consequently, specimens with missing parts (e.g., broken spines) should be excluded from analyses.

To reduce dimensionality and multicollinearity, a principal component analysis (PCA) was carried out on the three sets of morphological data matrices, using the princomp routine in R (R Core Team 2021). According to Blonder et al. (2014: [http://www.benjaminblonder.org/hypervolume\\_faq.html](http://www.benjaminblonder.org/hypervolume_faq.html)), high dimensionality can lead to hypervolumes with disjoint data points that can confound comparisons, owing to a lack of sufficient data points. Thus, for each set, three or four components necessary to explain > 80–90% of the total variance in the dataset were retained for further analysis. All hypervolumes were created using the Gaussian kernel density estimator method with the default Silverman bandwidth estimator (Blonder et al. 2014; Blonder 2018), with a 0% quantile threshold and 1000 Monte Carlo samples per data point. The bandwidth axis was estimated for each axis individually, using the estimate bandwidth function, which measures the trade-off between variance in the data and sample size (Blonder et al. 2016). After finding the intersection between the two hypervolumes, overlap values were calculated between individual pairs of taxa (2 x shared volume/summed volume) (Blonder et al. 2014). Comparisons between Euclidean distances from taxon hypervolume centroids were also made.

## 2.5. Phylogenetic analyses and species delimitation

Mesocoxal muscle tissue was excised from 34 *Holaptilon* specimens preserved in 96% ethanol. Total genomic DNA was extracted using the E.N.Z.A.<sup>®</sup> Tissue DNA Kit protocol for animal tissue. Four loci were targeted for amplification and sequencing: 16S ribosomal DNA (16S, 508 bp), Isocitrate dehydroxynase (IDH, 718 bp), histone 3 protein-coding for the nucleosome (H3, 330 bp), and cytochrome c oxidase I (COI, 658 bp). Primer sequences and amplification protocols for these four loci are provided in Table S5. PCR products were visualised using gel electrophoresis to confirm the correct amplification or detect undesired contamination. Amplicons

were purified with Thermo Scientific Exonuclease I and the FastAP Thermosensitive Alkaline Phosphatase Cleanup Kit. They were sequenced at MacroGen Europe with complements and sufficient overlap with adjacent regions to ensure accuracy of sequence data. Sequences were manually edited and aligned using Geneious R10 (<https://www.geneious.com>) for nucleotide editing and contig assembly. ClustalW (Thompson et al. 1994) was used to perform multiple sequence alignments of protein-coding genes on MEGA-X (Kumar et al. 2018), which was then converted to Fasta and Nexus formatted files for use in various analysis programs.

We analysed 34 *Holaptilon* individuals; GenBank accession numbers and sampling localities of specimens are listed in Table S1. In this study, three different datasets were used to analyse the phylogenetic relationship among *Holaptilon* groups. Dataset number one (1166 bp) contained the combined gene fragments of the COI barcode (658 bp) and 16S (508 bp) concatenated into two partitions. Dataset number two (1048 bp) contained the combined gene fragments of H3 and IDH concatenated into two partitions. Dataset number three (2214 bp) contained the combined gene fragments of all four mentioned genes concatenated into four partitions. A selection of specimens was sequenced for 18S (955 bp) and 28S (490 bp), but because these genes turned out to be (almost) invariable in *Holaptilon*, these sequences were not used for further analyses. All novel DNA sequences, i.e., 33 COI, 31 H3, 33 16S, 32 IDH, 5 18S, and 7 28S sequences, were deposited in GenBank (accession numbers OR536777–OR536809, OR541990–OR542033, OR545419–OR545480). *Gonypetyllis semuncialis* Wood-Mason, 1891 was chosen as outgroup for the phylogenetic analyses because this genus is morphologically similar to *Holaptilon* and it belongs to the same family (Gonypetidae) and subtribe (Gonypetyllina).

The best-fit model of nucleotide substitution for all sequences partitioned by gene, GTR+I+G for mitochondrial genes, and HKY for nuclear genes, were selected under the corrected Akaike Information Criterion (AICc; Hurvich and Tsai 1989) using jModelTest ver. 2.1.10 (Darriba et al. 2012). IQ-TREE 1.6 was used to perform a maximum likelihood (ML) phylogenetic tree estimation (Nguyen et al. 2015). In ten independent runs, 1000 ultrafast bootstrap replicates (UFBoot) (Hoang et al. 2018) and 1000 Shimodaira-Hasegawa approximate likelihood ratio test replicates (SH-aLRT) (Anisimova et al. 2011) were calculated. Bayesian analyses were conducted utilizing MrBayes v3.2.7 (Huelsenbeck and Ronquist 2001; Ronquist and Huelsenbeck 2003), employing the most suitable DNA substitution model under the Akaike Information Criterion (AIC). The analysis involved four chains, consisting of two hot and two cold chains, executed in three independent runs for 200,000,000 generations, sampling every 2000th generation. The first 20% of generations were discarded as burn-in. The majority-rule consensus tree was created using the “sumt” command. TRACER (Rambaut et al. 2018) was used to check that analysis has reached an effective sample size (ESS) over 200 in order to ensure correct chain con-

vergence. Posterior probabilities (pp) were obtained for each clade, where  $pp \geq 0.95$  indicated significant support for clades. The run with the best log-likelihood score was selected. Consensus trees generated were visualised in FigTree 1.4.2 (<http://tree.bio.ed.ac.uk/software/figtree>), and then edited using Inkscape vector graphics editors (ver. 1.2). Three different protocols, Assemble Species by Automatic Partitioning (ASAP) (Puillandre et al. 2021), Bayesian implementation of the Poisson Tree Processes model (bPTP) for species delimitation (Zhang et al. 2013), and the multi-rate PTP (mPTP) (Kapli et al. 2017) were used with pairwise genetic distances for species delimitation analyses. For ASAP, FASTA-configured files of all, nuDNA (H3, IDH), and mtDNA (COI, 16S) datasets were used for analyses on the ASAP website (<https://bioinfo.mnhn.fr/abi/public/asap>) with two replacement samples used to estimate distances, namely the simple p-distance model and the K2P model. bPTP was run on the bPTP online server (<https://species.h-its.org>) with default values (100,000 Markov chain Monte Carlo [MCMC] generations, thinning = 100, burn-in = 0.1, and seed = 123), using the NEXUS formatted input files of all, nuDNA (H3, IDH), and mtDNA (COI, 16S) datasets. The multi-rate PTP (mPTP) method was also used according to the study by Kapli et al. (2017) which incorporates the potential divergence in intraspecific diversity to the PTP and implements a fast method to compute the maximum likelihood delimitation from an inferred phylogenetic tree of the samples. The specific settings used in the mPTP analysis included a total of 100,000 MCMC generations, 10,000 generations as burn-in, and thinning every 100 generations. An uninformative prior was applied to the number of species, and the genetic model used was GTR+G. Species were delimited based on a threshold of 0.95 for posterior probabilities (<https://mptp.h-its.org>).

All 34 samples used for our molecular analyses were tested for an infection of the *Wolbachia* surface protein-coding gene (WSP, 549 bp) using the primer pair wsp81F (5'-TGG TCC AAT AAG TGA TGAAGA AAC-3') and wsp 691R (5'-AAA AAT TAA ACG CTA CTC CA-3') with the following PCR protocol: 95°C for 5 min, followed by 38 cycles at 95°C for 30 s, 55°C for 90 s, 72°C for 2 min, and terminated with a final extension step at 68°C for 30 min. The PCR products were loaded onto a 1.4% agarose gel and stained with GelRed (Biotium, Fremton, USA) to check for positive or negative infection. We included tests on *Wolbachia* to ensure that our molecular markers were not impacted by this entero-parasitic bacterium. *Wolbachia* can influence mitochondrial DNA (mtDNA) patterns, resulting in misleading phylogenetic signals among closely related species and specimens of the same species (Ritter et al. 2013). It can either obscure species diversity due to mtDNA introgression among species (Narita et al. 2006; Whitworth et al. 2007), or conversely, it can induce extensive mtDNA divergence due to prolonged reproductive isolation among lineages infected and not infected with *Wolbachia*, which may even lead to the formation of new species (Bordenstein et al. 2001).

## 2.6. Divergence dating analyses

We estimated the divergence time using BEAST 2 version 2.7.5 (Bouckaert et al. 2019). Two datasets were utilised: one from mitochondrial genes (COI, 16SrDNA) and another from nuclear genes (H3, IDH), which were concatenated to prevent coalescence and zero-length branches. Tree models were set as linked, the site model and clock model were set unlinked. The subsets and substitution models were determined using jModelTest version 2.1.10. For the mitochondrial dataset, the GTR model with estimated base frequencies and a gamma distribution (with 4 categories) was chosen. The nuclear dataset employed the HKY model with estimated base frequencies and the same gamma distribution setup. As fossils for *Holaptilon* or closely related genera are unavailable, the tree was calibrated using standard gene substitution rates as done in previous studies (Papadopoulou et al. 2010; Wendt et al. 2022). Consequently, a clock rate of 0.0177 was applied to the mitochondrial dataset, and 0.00177 to the nuclear dataset, using an optimised relaxed clock (Papadopoulou et al. 2010). To assess the potential effects of different models, two separate analyses were conducted using Yule and Birth-Death tree priors. Each analysis comprised four independent Markov Chain Monte Carlo (MCMC) runs, each running for 50 million generations and sampling trees every 5,000 generations. After discarding the initial 10% of trees as burn-in, convergence was verified using Tracer version 1.7.1 (Rambaut et al. 2018). The final trees were combined using TreeAnnotator v.1.10.4 and edited in FigTree v.1.4.4 (<http://tree.bio.ed.ac.uk>).

## 2.7. Biogeographic analyses

To study the historical shifts in the geographical ranges of *Holaptilon*, two models were used for biogeographical range expansion, the Dispersal-Extinction-Cladogenesis (S-DEC) model and the Dispersal-Vicariance (S-DIVA) model on RASP 4.3 (Yu et al. 2020). The input for this analysis was an ultrametric tree created using BEAST v2.7.5. To refine the analysis, the outgroup (*Gonypetyllis semuncialis*) was removed from the tree using the tool provided by the RASP software. Five geographical regions were here defined based on our understanding of the species current distribution: (A) south-western part of Iran, (B) north-western part of Iran, (C) Turkey, (D) north-eastern part of Iran, and (E) Israel/Jordan.

To address uncertainties arising from the tree's structures, all trees sampled from BEAST analysis, except for the initial 500 trees, were incorporated. For S-DIVA analysis, the "Allow Reconstruction" feature was selected, which allowed a maximum of 100 reconstructions utilising three random steps. This was followed by conducting up to 1000 reconstructions for the final tree. Each node in the analysis was granted the potential for up to four distinct areas. The outcomes of the most appropriate S-DIVA reconstructions were then summarised by employing the pruned maximum-clade-credibility tree derived from this Bayesian phylogenetic study. For S-DEC analysis,

the probability of dispersal between areas was considered as equal, and all values in the dispersal constraint matrix were set to 1 with four as the maximum number of areas.

## 2.8. Conservation evaluation

A brief and preliminary evaluation of the conservation status of each species was done referring to the IUCN Red List Categories and Criteria and Guidelines for Using the IUCN Red List Categories and Criteria (version 15.1, 2022). The aim of this analysis is to give a preliminary assessment that can be used as a base for a future standard IUCN Red List evaluation. The Extent of Occurrence (EOO) is defined as minimum convex in which no internal angle exceeds 180 degrees and which contains all sites of occurrence, the number of known presence locations, the presence of human activities or habitat degradation, and the fragmentation of populations, were considered to evaluate a Threat Level according with IUCN standards.

## 3. Results

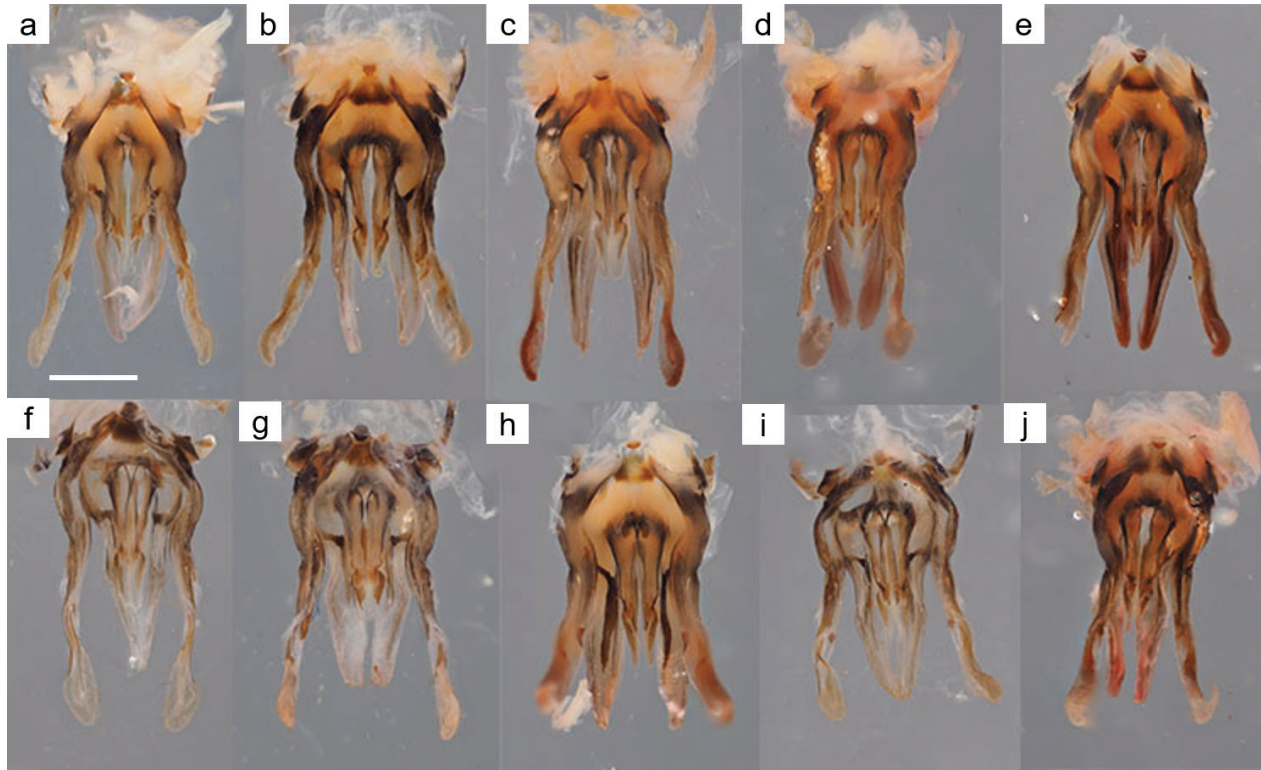
### 3.1. Genital morphology in females and males

The genitalia of 25 *Holaptilon* female and 30 male specimens were examined in this study. Some female genital characters (i.e., the shape of the gonapophyses, gonoplags, and gonocoxae) were proven to be useful in delimiting genera and species-level boundaries in some praying mantids (Brannoch and Svenson 2016). Our results showed that the female genitalia of the 25 analysed female specimens exhibited strong variability and weak discriminant differences in shape (Fig. 1).

A similar situation was obtained for male genitalia (25 males from Iran, including one paratype of *H. brevipugilis*, four males of *H. pusillum* from Israel, and photos of a single male's genitalia of *H. yagmur*; Yilmaz and Sevgili 2023). All specimens were grouped into seven morphotypes (Ha–Hg) based on the length and shape of **afa**, sclerotisation of **pba** anterior of **afa**, and the shape of the posterior edge of **vla** (Table 1). The Ha morphotype (11 specimens) is characterised by having long, saber-like **afa**, which has constant width and a gently curved or straight apex, **pba** anterior of **afa** is not sclerotised; posterior edge of **vla** is gently angular (Figs 2a and 2b). The Hb morphotype (5 specimens) is characterised by short, finger-like **afa**, which markedly narrows towards the apex and often is curved near it; **pba** anterior of **afa** is markedly sclerotised; posterior edge of **vla** is markedly truncated (Figs 2c and 2d). The Hc morphotype (2 specimens) is characterised by short, finger-like **afa**, with a curved apex, **pba** anterior of **afa** wholly sclerotised; posterior edge of **vla** is oblique (Figs 2e and 2f). The Hd morphotype (2 specimens) is characterised by short, finger-like

**Table 1.** Different morphotypes of *Holaptilon* species according to different characters of male genitalia.

Morphospecies	afa	afa apex	pba	vla
Ha	long, saber-like	constant width, a gently curved or straight apex	not sclerotized	gently angular
Hb	short, finger-like	markedly narrows towards the apex, often curved near it	markedly sclerotized	markedly truncated
Hc	short, finger-like	curved apex	wholly sclerotized	oblique
Hd	short, finger-like	gently curved apex	less sclerotized	oblique
He	very short, finger-like	curved at the apex	not sclerotized	oblique
Hf	long, hook-like	curved at the apex	strongly sclerotized	oblique
Hg	short, straight	straight apex	sclerotized	NA

**Figure 1.** Ventral view of the female genitalia of different *Holaptilon* species: **a, b** *H. abduallahii* sp. nov.; **c–e** *H. iranicum* sp. nov.; **f** *H. tadovaniensis* sp. nov.; **g** *H. brevipugilis*; **h–j** *H. khozestani* sp. nov.; scale bar: 300  $\mu$ m.

**afa** with a gently curved apex, **pba** anterior of **afa** less sclerotized; posterior edge of **vla** is truncated, but the truncation is not as clear-cut as in morphotype Hb (Figs 2g and 2h). The He morphotype (6 specimens) is characterised by very short, finger-like **afa**, which is curved at the apex, **pba** anterior of **afa** that is not sclerotised, with the posterior edge of **vla** oblique (Figs 2i and 2j). The Hf morphotype (3 specimens) is characterised by long, hook-like **afa** which is strongly sclerotised (Figs 2k and 2l). The Hg morphotype (1 specimen) is characterised by short, straight **afa**, **pba** anterior of **afa** is sclerotised (Yılmaz and Sevgili 2023). Note that all these differences may show intraspecific variability.

Taken together, the results point out to six groups of specimens that we treat as species: the Ha morphotype (= *H. abduallahii* sp. nov.), the Hb morphotype (= *H. iranicum* sp. nov.), the Hc morphotype (= *H. tadovaniensis* sp. nov.), the Hd morphotype (= *H. brevipugilis*), the He morphotype (= *H. khozestani* sp. nov.), the Hf morphotype (= *H. pusillulum*), the Hg morphotype (= *H. yag-*

*mur*), which will be properly described or redescribed in the section “Taxonomy”.

### 3.2. Other morphological features

Characteristics regarding the head, thorax, forelegs, and supra-anal plate of 51 adult specimens were examined and compared. *Holaptilon* species exhibited a generally homogenous morphology and the traditionally used morphological characters mentioned above all showed comparatively small differences. The only apparently constant differentiating character were the five posteroventral fore-femoral spines in *H. abduallahii* sp. nov., whereas all other species of *Holaptilon* seem to possess only four. The number of other spines in the forelegs of *Holaptilon* species is variable. Variability in the number of spines was also recorded in the left and right forelegs of the same individual (Table S2). As a result, it appears that the external morphology of the species in this genus is

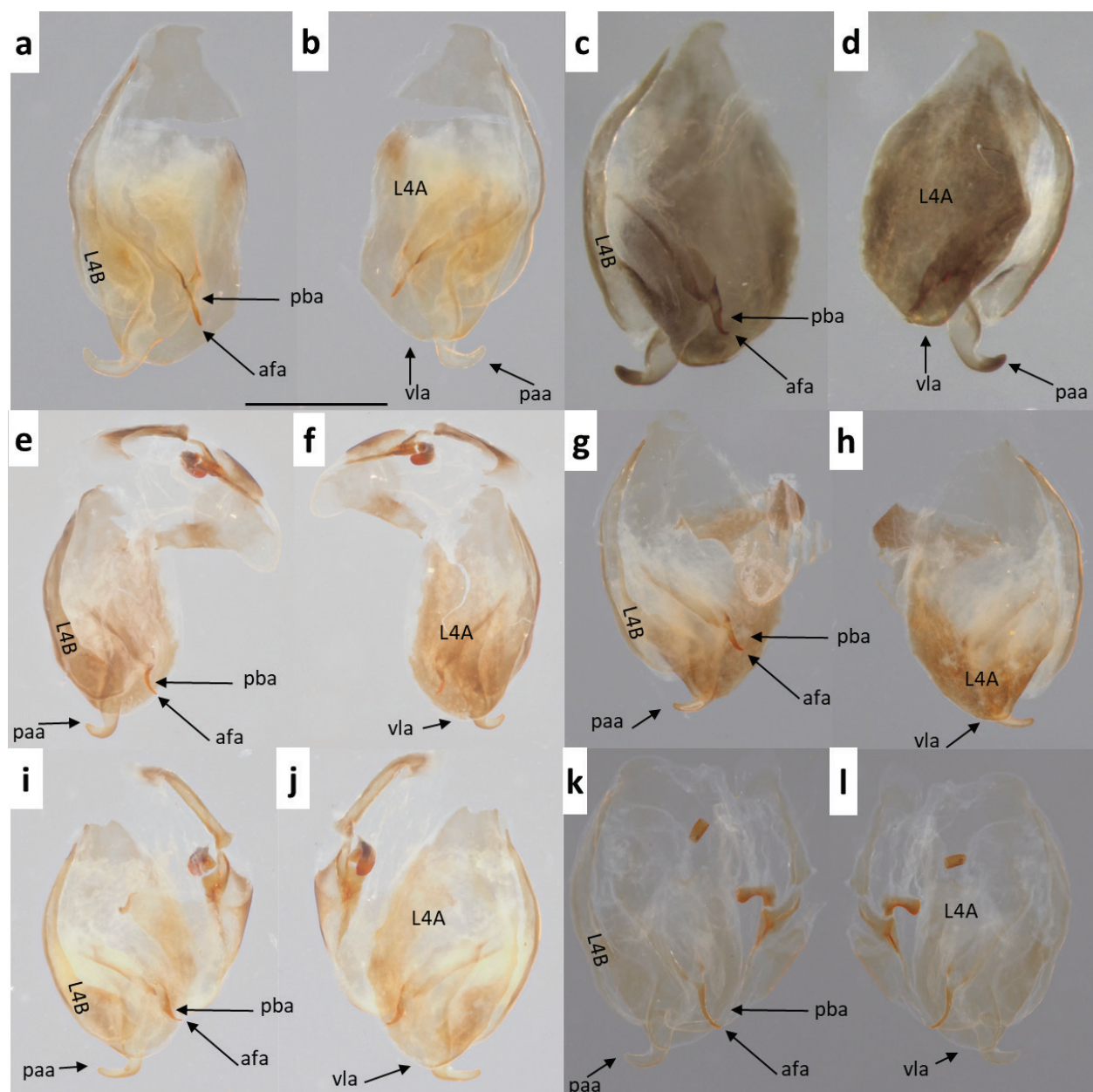


**Figure 2.** Dorsal view and ventral view of male genitalia of different *Holaptilon* species: **a, b** *H. abdullahii* sp. nov.; **c, d** *H. iranicum* sp. nov.; **e, f** ventral view *H. tadovaniensis* sp. nov.; **g, h** *H. brevipugilis*; **i, j** *H. khozestani* sp. nov.; **k, l** *H. pusillulum*; scale bar: 500  $\mu$ m. afa = anterior process (left phallic complex: left phallomere). paa = apical process (left phallic complex: left phallomere). vla = the right-posterior ventral lobe (left phallic complex: “ventral phallomere”; with L4A sclerotization in ventral wall; with opening of ejaculatory duct in dorsal wall). pba = (left phallic complex: left phallomere), of afa plus the edge (between pouches pne and lve) from which they arise (with L1 and L2 sclerotizations). L4B = sclerite extending over the dorsal wall (left phallomere). L4A = sclerite extending over the ventral wall (left and “ventral” phallomere).

highly variable and requires a multidisciplinary approach to understand its species boundaries. Therefore, the only morphological characters that are reliable as diagnostic characters for species are the number of posteroventral spines of the fore-femora and the characteristics of male genitalia.

### 3.3. Morphometric analysis

The morphometric ratios PL/HH and secondarily HH/HW were the most discriminative in both males and females

(Fig. S1). These ratios, when plotted together, demonstrated at least a clear separation between the taxon groups *iranicum* + *tadovaniensis* and *abdullahii* + *brevipugilis* + *pusillulum*, while the placement of *khozestani* within the latter group seemed to be more defined in males (Fig. S2). This indicates that the male individuals within the “*khozestani*” group tend to have distinct or well-defined values for morphometric ratios compared to males from other taxon groups. On the other hand, the females within the “*khozestani*” group might have more overlapping values with females from other groups, making it somewhat more difficult to clearly distinguish them based on these

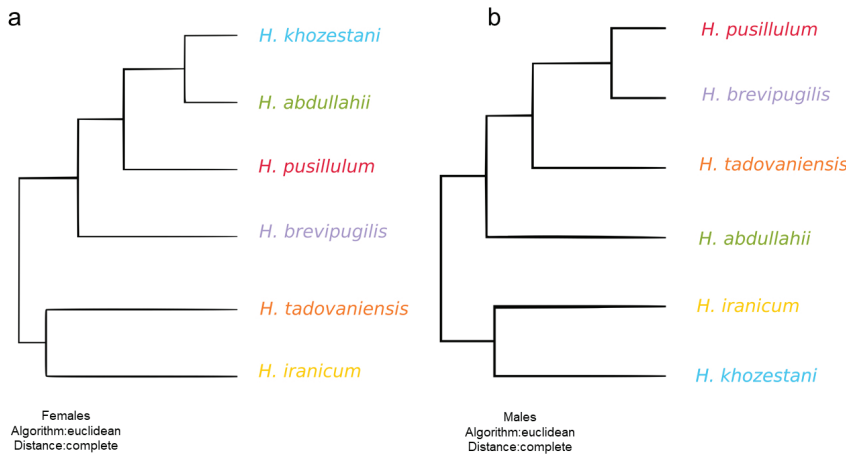


**Figure 3.** Cladistic dendrogram with complete linkage and euclidean distance ([https://www.bioinformatics.com.cn/plot\\_basic\\_dendrogram\\_plot\\_018](https://www.bioinformatics.com.cn/plot_basic_dendrogram_plot_018)) for morphometric parameters of different species of females (a) and males (b) of *Holaptilton* species.

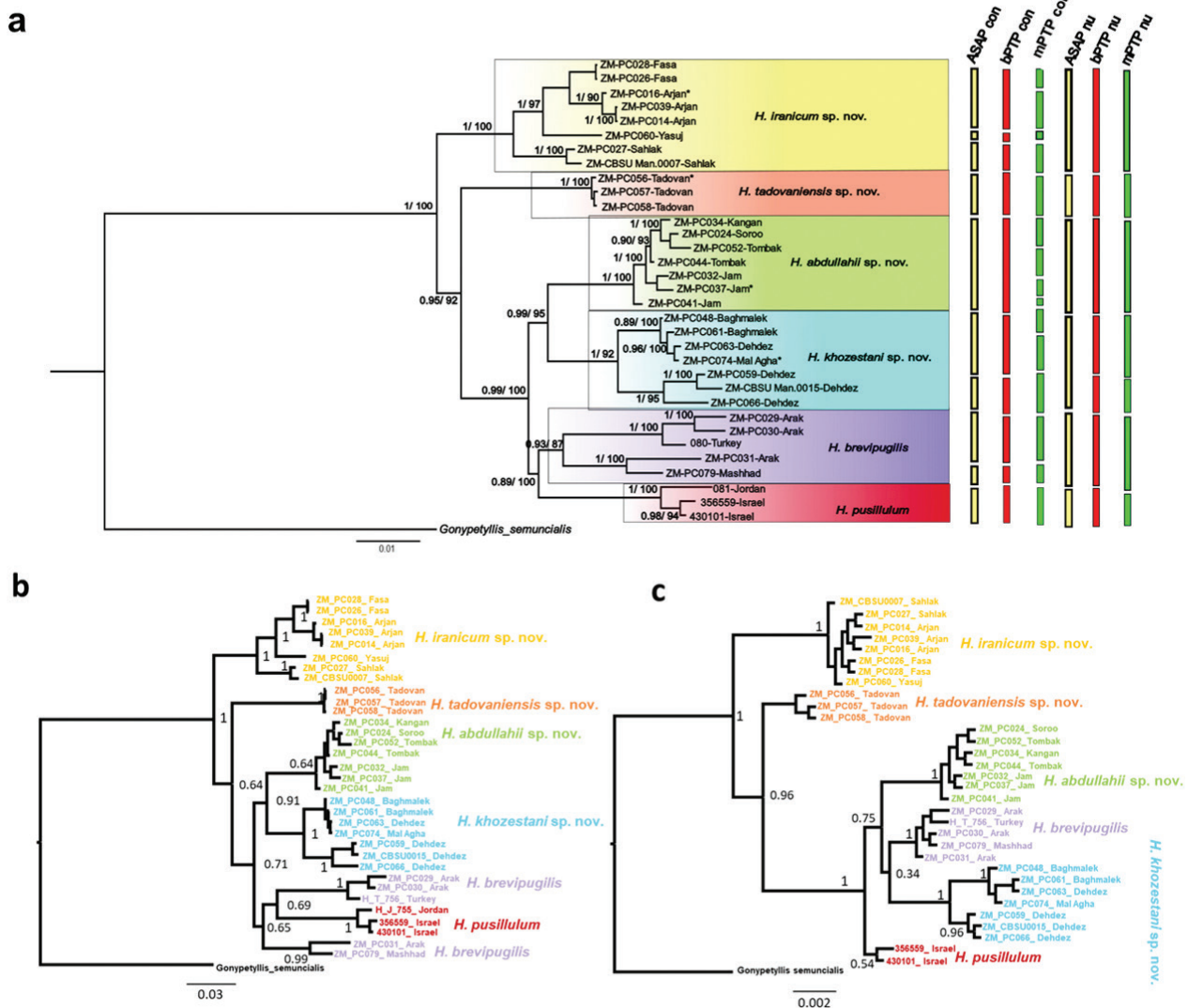


**Figure 4.** Phylogenetic trees of *Holaptilton*: **a** Phylogeny and Molecular Species Delimitation of the genus *Holaptilton* using a combined phylogenetic tree made through Bayesian (BI) and Maximum Likelihood (ML) approaches with the utilization of MrBayes and IQ tree, respectively (both trees did not differ in their topology) based on concatenated COI, 16S rRNA, H3, and IDH sequences, showing the phylogenetic placements of the new samples from Iran and results of three molecular species delimitation methods, ASAP: Assemble Species by Automatic Partitioning; bPTP: Bayesian implementation of the PTP model for species delimitation; mPTP: multiple-rate Poisson Tree Process. Support values are indicated beside the nodes [BI posterior probability/ML bootstrap (PP/BP)], holotypes are marked with asterisks (\*); con: concatenated, nu: nuDNA. The BI tree was used as the basis for this figure. **b** Phylogenetic tree made using Bayesian (BI) method of the genus *Holaptilton* based on concatenated COI and 16S rRNA sequences; **c** Phylogenetic tree made using Bayesian (BI) method of the genus *Holaptilton* based on concatenated H3 and IDH sequences.

specific morphometric ratios. The dendrogram, at least for females, was very similar to the molecular phylogeny (Fig. 3), supporting, despite the evident variability, the existence of separate lineages inside the genus *Holaptilon*. While *H. iranicum* seemed quantitatively well separated from the type species *H. pusillum*, the boundaries among the other species were less well defined using only traditional morphology, but the integration of the dendrogram using morphometric ratios (Fig. 3) with the results of the analysis of molecular data (Fig. 4) in this study advanced our understanding of the phylogenetic relationships among the investigated taxon groups. By employing discriminative morphometric ratios (PL/PW and HH/HW), clear distinctions were observed between the groups “*iranicum* + *tadovaniensis*” and “*abdullahii* + *brevipugilis* + *pusillum*” with potential sexual dimorphism in the “*khozestani*” group. The integrative analysis demonstrated a concordance between morphometry-based and genetic-based groupings, providing compelling evidence for the validity of taxonomic distinctions and emphasising the importance of considering both data types for accurate phylogenetic inferences. For all these considerations, a traditional dichotomous key for species identification, based on morphology alone may be misleading for this genus. A key to the species is however here proposed to give a preliminary help for faunistic studies and general field work.

### 3.4. Morphological hypervolume

In total, five species were included in the analysis: *H. abdullahii* sp. nov. (N = 20 specimens), *H. khozestani* sp. nov. (N = 13), *H. brevipugilis* (N = 4), *H. iranicum* sp. nov. (N = 11), *H. tadovaniensis* sp. nov. (N = 3). The morphological hypervolumes showed low levels of overlap among species (Figs S3, S4; Tables S6, S7), with the lowest overlap between *H. tadovaniensis* sp. nov. and *H. iranicum* sp. nov. and the highest overlap between *H. khozestani* sp. nov. and *H. abdullahii* sp. nov. followed by *H. brevipugilis* and *H. khozestani* sp. nov. Species had the highest overlap with set 1 estimated with three principal component axes, and the lowest with set 3 estimated with four principal component axes. In our study, some species were represented by numerous individuals while others only by few individuals, due to the difficulty finding the specimens in their natural habitat. The number of specimens in each population or sample is a critical factor in analysing morphological variation and interpreting results, especially in analyses of morphological hypervolumes. Sample size can influence the robustness of conclusions and the amount of variation observed. The differences in sample sizes therefore have to be always considered in the interpretation of our results.

### 3.5. Molecular phylogenetic analyses

Our test for *Wolbachia* infection proved negative for all our 34 *Holaptilon* samples used in the molecular study,

so we did not find evidence for an effect of *Wolbachia* infection on the phylogeny of *Holaptilon*.

All applied phylogenetic methods (Bayesian, Maximum likelihood) resulted in trees that did not differ much in their topology (Fig. 4), i.e., all groups of specimens were mostly assigned to the same main clades, and the relationships between these clades were mostly identical, except for the BI tree obtained using mitochondrial genes (COI, 16S), which suggests that *H. brevipugilis* might not form a monophyletic group. It is important to note that this latter relationship lacks robust support based on Bayesian analysis (Fig. 4b).

The *H. iranicum* clade in all three trees represented the first split and was sister to the clade *H. tadovaniensis* + all other *Holaptilon* taxa. The *H. pusillum* clade remained the sister clade to the *H. brevipugilis* clade in the trees based on mitochondrial genes (COI, 16S) and the combination of all four genes (COI, 16S, H3, IDH), but was sister to the clade *H. abdullahii* and *H. brevipugilis* + *H. khozestani* in the tree based on nuclear genes (H3 and IDH). One combined tree (from ML tree and BI tree, which were identical in topology but with different support values) with well-supported nodes is given in Figure 4. The new species were resolved as monophyletic. Most of the nodes were well supported (0.89/90–1/100), and all taxa were resolved as independent lineages with long branches and they clearly belong to different clades than the type species *H. pusillum*.

The number of species defined by the species delimitation software for mtDNA and all markers combined were even higher than our assumptions above, i.e., ASAP multilocus (Kimura): ten species; bPTP multilocus: 14 species; mPTP multilocus: ten species. However, restricting the data to the nuDNA markers (H3, IDH) resulted in almost the same number of species as in our assumptions given above, ASAP: 6 species, bPTP and mPTP: 7 species (Fig. 4).

### 3.6. Divergence dating, biogeography, and evolution analysis

Our molecular dating based on concatenated mtDNA (COI, 16S) and nuDNA (H3, IDH) datasets suggested that the most recent common ancestor of *Holaptilon* likely lived in the late Miocene, 8.4–6.1 Mya (Fig. 5b). The first divergence event in *Holaptilon* occurred approximately 6.06 Myr ago when the clade containing *H. iranicum* branched off from the rest of the *Holaptilon* group. Around 5.5 Mya, the clade containing *H. tadovaniensis* split off from all remaining *Holaptilon* taxa. Roughly 3.7 Mya, the split between the two sister clades *H. abdullahii* + *H. khozestani* and *H. brevipugilis* + *H. pusillum* occurred.

Since the biogeographic analyses results were consistent for both the S-DIVA and S-DEC methods, one of them was utilised (Fig. 5a). The model assumed an origin in south-western Iran (A) with range expansion to the north-western part of Iran (B) and Israel/Jordan (E) starting 3.7 Mya. They separated from A to BE (dispersion)

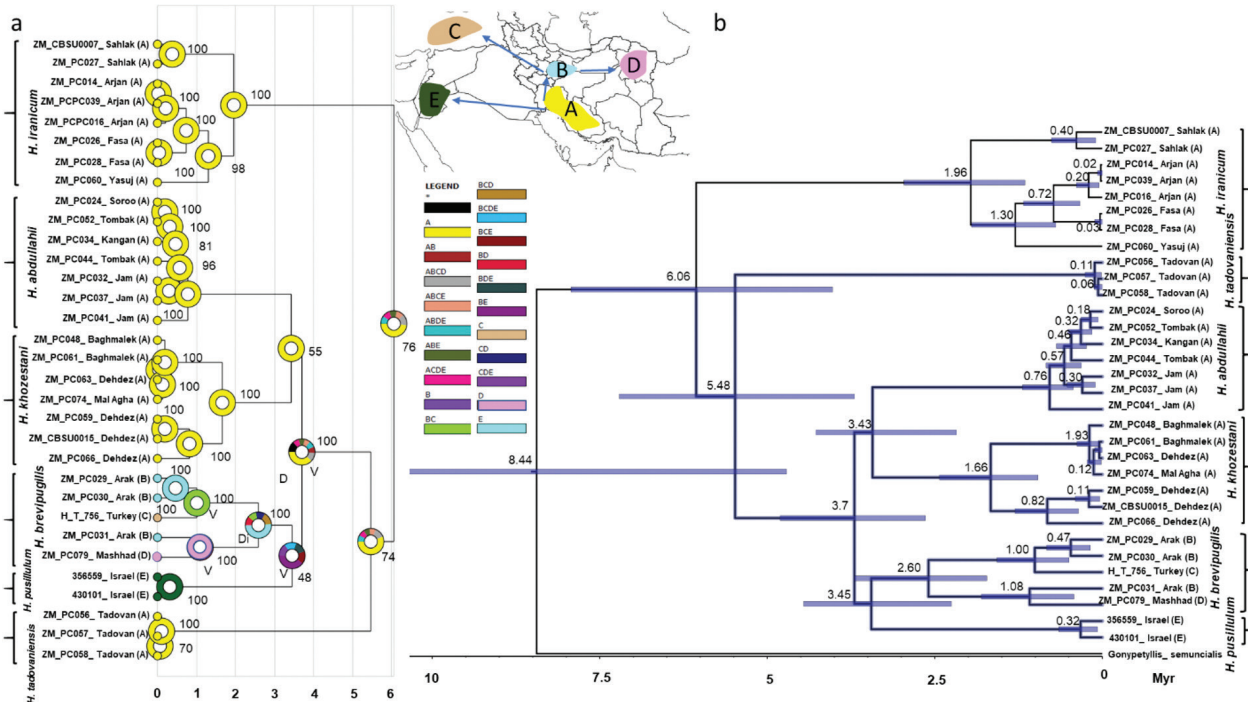


**Figure 5.** **a** Ancestral range estimation of *Holaptilon*. The biogeographic reconstruction combination of RASP S-DIVA and S-DEC biogeographical analysis models (max. number of areas = 3). The pie charts indicate alternative ancestral geographical ranges and their probabilities. The pie charts on the descendant branches show the ranges immediately after the speciation event, whereas the pie charts on the nodes display the range changes along branches before speciation events. Numbers besides the pie charts are for the ancestral range that received the highest probability. Species were assigned to the five distribution areas A to E as illustrated on the inset map and the respective tip ranges (coloured squares with letter codes at tips). The legend below the inset map displays the colour codes for each area, including the area combinations as retrieved in the analysis. D = dispersal, V = vicariance events were shown as Di or V under the pie charts. **b** Phylogeny and diversification of *Holaptilon* based on a four-locus (COI, 16S rDNA, H3, IDH) species tree constructed in \*Beast. 95% posterior probability confidence intervals are shown with blue bars.

between 3.7 and 3.4 Mya, and then separated into B and E (vicariance), starting about 3.4 Mya. E remains stable with no changes until today. From B, the taxon expanded its range moving to BD and BC (dispersion), starting about ~2.8 Mya to ~1.0 Mya. In the last ~1My, two distinct vicariant events occurred, which separated B, C, and D into distinct areas (Fig. 5a).

Today, several species (i.e., *H. iranicum*, *H. tadovaniensis*, *H. khozestani*, *H. brevipugilis*) occur together in the Zagros Mountains forest steppe ecoregion (Dinerstein et al. 2017). Among these species, *H. brevipugilis* exhibits the widest distribution, spanning three ecozones, namely the Eastern Mediterranean conifer-broadleaf forests, the Zagros Mountains forest steppe, and the Central Persian desert basins. Conversely, *H. abdullahii* and *H. pusillum* are confined to the South Iran Nubo-Sindian desert and semi-desert, and the eastern Mediterranean conifer-broadleaf forests, respectively. Although *Holaptilon* mantids have a vast geographical distribution

(extent of occurrence EOO: approximately 1.5 Mio km<sup>2</sup>), encompassing four different ecoregions, they are often encountered in fragmented and scarce populations. Their places of occurrence frequently deviate from the typical vegetational pattern of the overall ecoregion but exhibit certain consistent microecological features, such as rocky grounds sparsely covered by vegetation, sometimes near water streams. Notably, these habitats are often found within non-natural or modified environments, such as cultivated fields or urban areas (Figs 6–8).

While five of the six species (i.e., *H. abdullahii*, *H. iranicum*, *H. khozestani*, *H. pusillum*, *H. tadovaniensis*) as far as known today have well-defined and restricted distributions, only *H. brevipugilis* has a vast but possibly fragmented distribution spanning 20 degrees of longitude (39–59°E) across the Middle East, while most likely maintaining a relatively narrow latitudinal range (34–37°N). This large distribution of *H. brevipugilis* may encompass regional subspecies.

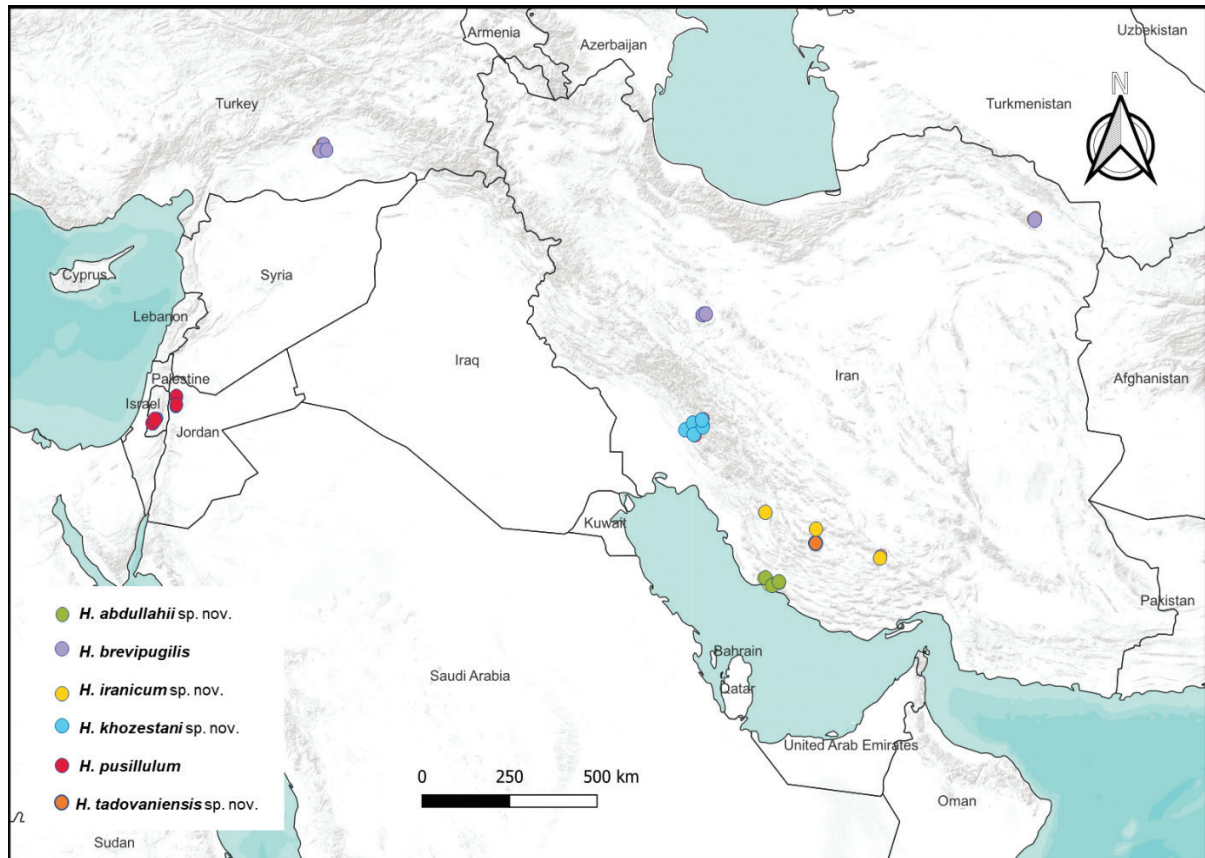


Figure 6. Current and historic records of *Holaptilon* species, visualisation with QGIS v. 3.22, Base map: ESRI Terrain map.

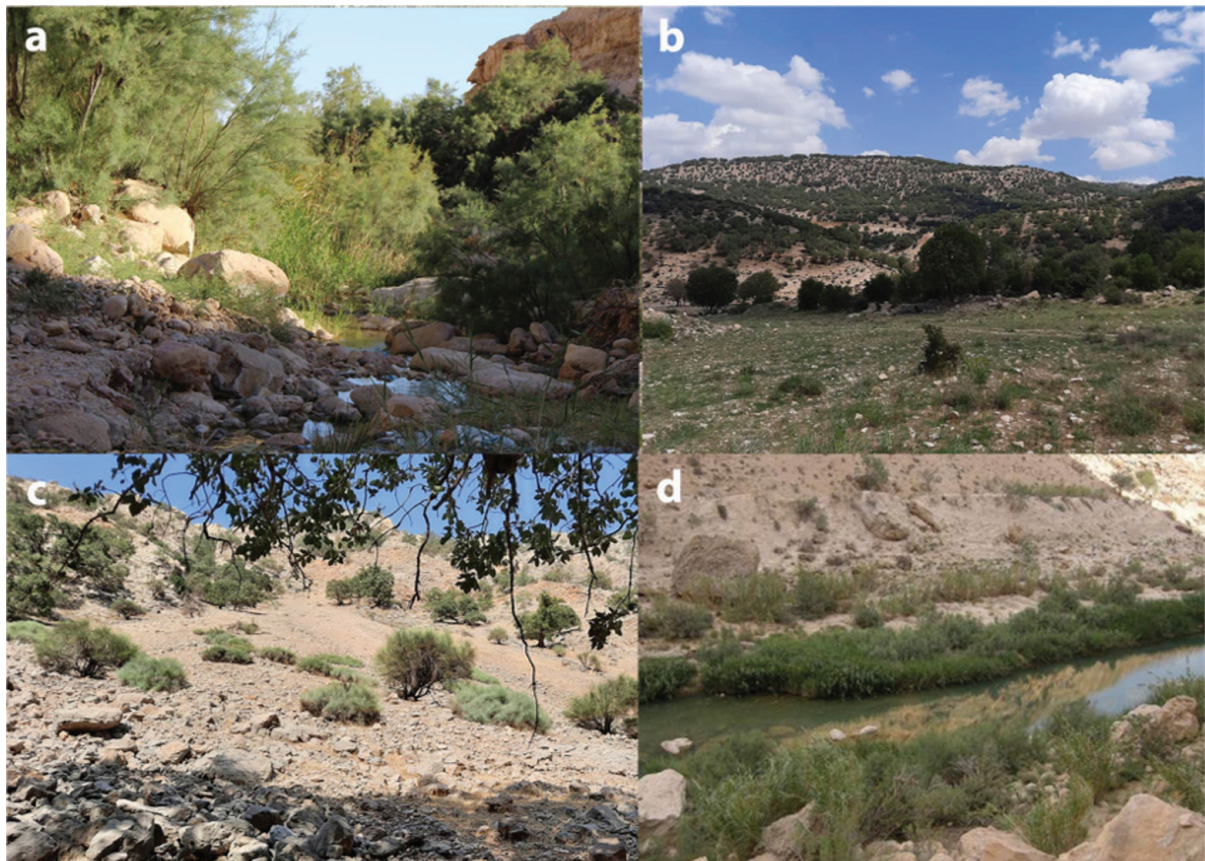


Figure 7. Examples of the habitats of *Holaptilon* species: **a** *H. abdullahii* sp. nov., Soroo, Busheher province (29.569N, 51.947E). **b** *H. iranicum* sp. nov., Arjan, Fars province (29.569N, 51.947E). **c** *H. khozestani* sp. nov., Malagha, Khozestan province (31.607N, 49.998E). **d** *H. tadovaniensis* sp. nov., Tadovan, Fars (28.853N, 53.326E).



**Figure 8.** Levels of urbanization and degradation of natural habitats at collection sites of two *Holaptilon* species: *H. pusillulum* (red circles) and *H. brevipugilis* (red stars). **a** As-Salt, Jordan (32.046N, 35.737E). **b** Anjara, Jordan (32.301N, 35.764E). **c** Wadi Fukin, Jerusalem (31.702 N, 35.099 E). **d** Mashhad, Iran (36.316N, 59.410E). **e** Siverek, Turkey (37.768N, 39.797E). **f** Haftad Qolleh Protected Area, Markazi Province, Iran (34.133N, 50.217E) scale 1:6000, base map: Google satellite map.

## 4. Taxonomy

**Order:** Mantodea

**Family:** Gonypetidae Westwood, 1889

**Tribe:** Gonypetini Westwood, 1889

**Subtribe:** Gonypetyllina Schwarz & Roy, 2019

**Genus:** *Holaptilon* Beier, 1964

### 4.1. Key to *Holaptilon* species

- 1 Femora with 5 posteroventral femoral spines (southern Iran) ..... *abdullahii* sp. nov.
- 1' Femora with 4 posteroventral femoral spines ..... 2
- 2 Ratio of HH/HW to PL/HH less than 0.6 ..... 3
- 2' Ratio of HH/HW to PL/HH greater than 0.6 ..... 5
- 3 (restricted to Israel and Jordan) ..... *pusillulum*
- 3' (restricted to southern Iran) ..... 4
- 4 afa short, finger-like, markedly narrowed towards apex and often curved near it ..... *iranicum* sp. nov.
- 4' afa short, finger-like, less markedly narrowed towards apex, curved ..... *tadovaniensis* sp. nov.
- 5 Posterior edge of vIa truncated (restricted to south-western Iran) ..... *khozestani* sp. nov.
- 5' Posterior edge of vIa oblique (not in southern Iran) ..... *brevipugilis*

### 4.2. Genus *Holaptilon*

**Type species.** *Holaptilon pusillulum* Beier, 1964.

**Redescription.** Small size (11–23 mm), both sexes apterous. Head thick, wider than pronotum, with rounded apex. Lower frons wider than high. Compound eyes glob-

ular; ocelli rounded, bigger in males, the third ocellus in the centre is smaller than the other two in both sexes; vertex rounded and more or less convex. Lower frons two times wider than high. Antennae filiform, ciliated in both sexes. Pronotum flat with some more or less pronounced dorsal bulges, short and compressed, almost entirely oval, only slightly incurved at the anterior margin and truncate at the posterior margin, lateral margin dentated with some setae and irregular black spots. The supra-coxal sulcus strongly bold and curved separating the prozone part from the metazone part. Prozone stout and arched; metazone slightly longer than prozone, with three different sized gibbositities on each side of supra-coxal sulcus. Meso- and metatergum a little different from abdominal tergites, a bit longer, finely keeled along midline, with posterior margin more or less inward curved. Forelegs stout, the coxae widely surpassing the prosternum posteriorly, very weakly spined, with divergent lobes and black coloured in the anterior side; femora broad, with curved dorsal margin, four or five short posteroventral spines, four discoidal spines, the 1st extremely short, and a variable number of anteroventral spines more or less developed, 9–13; tibiae with very variable number of anterior spines, 10–13. Anterior side of forelegs variably coloured with reddish anteroventral area and back anterodorsal area with more or less developed black spot patterns. Tarsus slightly broadened distally and slightly flattened. Meso- and metafemora distinctly thickened basally. Meso- and metathoracic legs long and slender with fine setae, coxae shiny blue-black; the rest of legs yellowish, ciliated, with some small black spots on their posterior view; femora clearly thickened in the first part, with rounded genicular lobes, each bearing a single short apical spine. Tibiae with two tibial spurs. Abdomen slender, tergites weakly keeled. Supra-anal plate wider than long, nearly triangular but with variably rounded apex. Cerci short, rotund, only slightly surpassing supra-anal plate. Male subgenital plate with styli.

#### 4.3. *Holaptilon pusillum* Beier, 1964

Figure 9k, l

**Type locality.** Yad Vashem near Jerusalem, Israel.

**Material examined.** 1♀, ethanol, Judean Hills, Ora, Yad VaShem, Israel, 31.774N, 35.175E, 8/1971, leg. Wahrman; 1♂, ethanol, Judean Hills, Qiryat Yearin, Israel, 31.802N, 35.099E, 5/2022, leg. More Yosef; 1♂, 1♀, ethanol, Judean Hills, Jerusalem, Israel, 31.768N, 35.157E, 8/1974, leg. Wahrman; 1♀, ethanol, Judean Hills, Ora, En Kerem, Israel, 31.774N, 35.175E, 8/1971, leg. Wahrman (SMNHHTAU).

**Remarks.** Since the only *Holaptilon* species occurring in Israel is *H. pusillum* and the material in SMNHHTAU was mostly collected at or close to the type locality, non-type material of this species was loaned from SMNHHTAU to prevent any damage to the type material.

The original description (Beier 1964) was based on only three specimens of the single-known *Holaptilon*

species at that time and cannot be used anymore to separate this species from the others. A new species diagnosis is therefore proposed, based on male genitalia here described for the first time.

**New diagnosis.** Males of this species can be distinguished from other *Holaptilon* species by the long, hook like **afa**, which is strongly sclerotised; posterior edge of **vla** oblique (Fig. 2k, l).

**Redescription.** Males are smaller and more delicate in appearance than females, both male and female apterous, head and body dorsally sandy brown, with small dark brown and black spots, mostly in the middle of body parts.

**Head:** Wider than high (ratio: 1.1–1.4), wider (ratio: 1.2) than pronotum (Table S3). **Pronotum:** Rectangular shape, almost flat, compact. Slightly higher than wide (ratio: 1.3) **Meso- and metanotum:** roof-shaped and keeled.

**Forelegs:** Femora broad, dorsal edge lamellar, two times longer than wide, armed with 11–12 anteroventral spines with the second one longer than the others; 4 discoidal spines with the first one shorter, the third one longer than the others, the second one is a bit smaller than the third one, the fourth is short but longer than the first one; 4 posteroventral spines, with the first one slightly longer than the other three spines, the first two spines are close to each other but the third and fourth are a bit more distant; anterior genicular lobe and posterior genicular lobe with a spine; foretibia armed with 9–10 anteroventral spines, elongating distally, and 11–13 posteroventral spines, also elongating distally (Fig. 12c). **Abdomen:** Slender but half as wide in male compared to female, the tergites weakly keeled in midline; supra anal plate transverse, triangular; cerci with nine readily recognizable cercomeres, covered by long setae; last cercomere longer and narrower than the others; subgenital plate much longer than wide. **Male genitalia:** Ventral phallomere oval, moderately wide; **afa** long, hook like, which is strongly sclerotised; posterior edge of **vla** oblique, **pba** anterior of **afa** sclerotised. Posterior edge of **vla** gently angular and not well sclerotised. Sclerite **L4B** curved, of complex shape, widened distally. Apical process **paa** long, directed left side, with curved apex (Fig. 2k, l). **Ootheca:** unknown.

**Measurements (in mm).** Body length: ♂ 11–12, ♀ 14–18; Head width: ♂ 2.7–3.0, ♀ 3.2–3.5; Head height: ♂ 2.3, ♀ 2.5–3.0; Pronotum length: ♂ 3.0, ♀ 3.0–3.7; Pronotum width: ♂ 2.3–2.4, ♀ 2.3–2.5; Forecoxa length: ♂ 2.0–2.8, ♀ 2.8–3.0; Forefemora length: ♂ 2.8–3.2, ♀ 3.0–3.8; Forefemora width: ♂ 1.3–1.5, ♀ 1.5–1.7.

**Distribution.** Israel, Jordan, and Palestine (Beier 1964; Fig. 6, red points).

**Conservation.** This species seems very localised with an Extent of Occurrence (EOO) of about 900 km<sup>2</sup> in a very limited number of locations. This species has been observed discontinuously from its original description in the middle of the 20th century probably because of not very abundant populations, cryptic habits and fragmented

populations. The anthropogenic presence and impacts in its habitats are variable but often heavy, involving different urban and agricultural land uses (fig. 8) with severe threats to the natural ecosystems; therefore, this species can be classified as Endangered (B2ab).

#### 4.4. *Holaptilon abduallahii* Mirzaee and Battiston sp. nov.

<https://zoobank.org/B82D6323-BEC7-43FB-A6FC-9130B3522BE6>

Figure 9a, b

**Material examined.** Holotype: 1♂, ethanol, with genitalia in a separate micro-vial, Jam, Bushehr province, Iran, 27.883N, 52.354E, 743 m, 11/2020, leg. Mirzaee (SDEI). — Paratypes: 3♀, ethanol, with genitalia in a separate micro-vial, Tombak, Bushehr, Iran, 27.726N, 52.209E, 83 m, 7/2015, 8/2016, 8/2019, leg. Abdullahi and Mirzaee (SDEI); 5♂, 3♀, 2 nymphs, ethanol, Tombak, Bushehr, Iran, 27.726N, 52.209E, 83 m, 7/2015, 7/2016, 7/2017, 5/2018, leg. Abdullahi and Mirzaee (ZMPC); 2♂, 4♀, ethanol, Tombak, Bushehr, Iran, 27.726N, 52.209E, 83 m, 8/2016, 8/2019, 8/2020, 8/2021, leg. Abdullahi and Mirzaee (ZMCB-SU); 2♂, ethanol, Tombak, Bushehr, Iran, 27.726N, 52.209E, 83 m, 7/2017, 8/2017, leg. Abdullahi and Mirzaee (ESPC); 2♂, 3♀, ethanol, Kangan, Bushehr, Iran, 27.843N, 52.064E, 57 m, 8/2019, 5/2020 leg. Abdullahi and Mirzaee (ZMPC); 3♂, 1♀, 1 nymph, ethanol, Jam, Bushehr, Iran, 27.883N, 52.354E, 83 m, 7/2019, 7/2020, leg. Abdullahi and Mirzaee (ZMPC); 1♂, ethanol, Soroo, Bushehr, Iran, 28.006N, 51.908E, 47 m, 4/2021, leg. Mirzaee (ZMPC).

**Diagnosis.** Males and females of this species can be distinguished from other species by having five posteroventral femoral spines and long, saber-like **afa** with a constant width that is gently curved or straight. Processes **pba** anterior of **afa** is not sclerotised, and the posterior edge of **vla** is gently angular (Fig. 2a, b).

**Description.** Males are smaller and more delicate in appearance than females, both male and female apterous, head and body dorsally sandy brown, with small dark brown and black spots, mostly in the middle of body parts. **Head:** Wider than high (ratio: 1.1–1.3), two times wider (ratio: 2) than pronotum (Table S3) (Fig. 10a, b). **Pronotum:** Rectangular shape, almost flat, compact. Slightly higher than wide (ratio: 1.2) **Meso- and metanotum:** roof-shaped and slightly keeled (Fig. 11a, b). **Forelegs:** Femora broad, dorsal edge lamellar, 1.8 times longer than wide, armed with 12 or 13 anteroventral spines, of which the second spine is longer than the others and the spines with even numbers are longer than spines with odd numbers; four discoidal spines with the first being shorter, the third longer than the others, the second a bit shorter than the third (both extrovertedly curved), the fourth is short but longer than the first; five posteroventral spines, with almost all of them of the same size, the first two spines are close to each other but the third and fourth are more distant and the fifth spine has a much greater distance and is far away from the other spines; anterior genicular lobe

and posterior genicular lobe with a spine; foretibia armed with nine or ten anteroventral spines, elongating distally, and 11, 12 or 13 posteroventral spines, elongating distally. The first three tarsomeres in most of the individuals (N = 21) blackish and the tarsomere number 4 and 5 white, in other individuals (N = 10) whole 5 tarsomeres white (Fig. 12e). **Abdomen:** Slender but half as wide in male compared to female, the tergites weakly keeled in midline; supra anal plate transverse, triangular; cerci with nine readily recognizable cercomeres, covered by long setae; last cercomere longer and narrower than the others; subgenital plate much longer than wide. **Male genitalia:** Ventral phallomere oval, moderately wide; **afa** long and saber-shaped, with constant width, gently curved or straight, strongly sclerotised in left half, **pba** anterior of **afa** not sclerotised. Posterior edge of **vla** gently angular and well sclerotised. Sclerite **L4B** curved, of complex shape, widened distally. Apical process **paa** long, directed left side, with curved apex (Fig. 2a, b). **Ootheca:** Dark yellow to creamy in colour, oval-shaped in dorsal view, dorsoventrally flattened. Rows of egg chambers that are parallel to the top and bottom of the egg, casing is visible from outside (Fig. 13a).

**Measurements (in mm).** Body length: ♂ 12–13, ♀ 15–20; Head width: ♂ 3.1–3.4, ♀ 3.5–4.0; Head height: ♂ 1.4–1.7, ♀ 1.7–2.0; Pronotum length: ♂ 2.7–3.2, ♀ 3.0–3.7; Pronotum width: ♂ 2.4–2.7, ♀ 2.5–3.1; Forecoxa length: ♂ 3.0–3.3, ♀ 3.0–3.6; Forefemora length: ♂ 3.2–3.5, ♀ 3.5–4.0; Forefemora width: ♂ 1.3–1.7, ♀ 1.7–2.2.

**Distribution.** South of Iran, Bushehr province (Jam, Kangan, Tompak, Soroo) (Fig. 6: green points).

**Habitat.** Rocky habitats within mountains where a permanent water source is available (Fig. 7a).

**Conservation.** This species seems very localized with an Extent of Occurrence (EOO) of about 300 km<sup>2</sup> in a small number of locations (4). With no data on population trends over time, and despite its natural habitat susceptible to low anthropogenic impacts, this species might have to be categorized as endangered, but further studies are necessary to clarify its threat status.

**Etymology.** Named after the first collector, Hossein Abdullahi.

#### 4.5. *Holaptilon brevipugilis* Kolnegari, 2018

Figure 9i, j

*H. yagmur* Yılmaz and Sevgili, 2023: 18. **new. syn.**

**Material examined.** Paratypes: 1♂, 1♀, ethanol, with genitalia in a separate micro-vial, Arak, Markazi province, Iran, 34.128N, 50.072E, 1803 m. 7/2018, leg. Kolnegari (SDEI). — Other material: 1♀ etha-

nol, Arak, Markazi province, Iran, 34.128N, 50.072E, 1803 m. 7/2018, leg. Kolnegari (SDEI); 1♂, ethanol, Mashhad, Khorasan Razavi, Iran, 36.316N, 59.410E, 995 m. 8/2021, leg. Ghafarnia (ZMPC), 1 nymph, Siverek, Karabahçe, Turkey, 37.776N, 39.735E, 08/2019, leg. K. Yılmaz and M. Yalçın (HSPC).

**New diagnosis.** Short **afa**, which is finger-like, less markedly narrowed towards apex, curved; **pba** anterior of **afa** less sclerotised; posterior edge of **vla** oblique (Fig. 2g, h).

**Redescription.** Males are smaller and more delicate in appearance than females, both male and female apterous, head and body dorsally sandy brown, with small dark brown and black spots, mostly in the middle of body parts. Head: Wider than high (ratio: 1.2–1.3), wider (ratio: 1.1) than pronotum (Table S3, Fig. 10i–l). Pronotum: Rectangular shape, almost flat, compact. Slightly higher than wide (ratio: 1.1) Meso- and metanotum: roof-shaped and slightly keeled (Fig. 11i–l). Coxae robust, shiny blue-black in some of the individuals but in some others not shiny black or only 1/3 black, anterior and posterior margin with some tubercles and setae. Femora broad, dorsal edge lamellar, two times longer than wide, armed with 10–12 anteroventral spines with the second one longer than the others; 4 discoidal spines with the first one shorter, the third one longer than the others, the second one is a bit smaller than the third one, the fourth is short but longer than the first one; 4 posteroventral spines, with the first one slightly longer than the other three spines, the first two spines are close to each other but the third and fourth have a bit more distance between them; anterior genicular lobe and posterior genicular lobe with a spine; foretibia armed with 9 anteroventral spines, elongating distally, and 10–13 posteroventral spines, also elongating distally (Fig. 12c). **Abdomen:** Slender but half as wide in male compared to female, the tergites keeled in midline; supra anal plate transverse, triangular; cerci with eight readily recognizable cercomeres, covered by setae; last cercomere longer and narrower than the others; subgenital plate much longer than wide. **Male genitalia:** Ventral phallomere oval, moderately wide; **afa** short, which is finger-like, less markedly narrowed towards apex, curved; **pba** anterior of **afa** less sclerotised. posterior edge of **vla** oblique; sclerite **L4B** curved, of complex shape, widened distally. Apical process **paa** long, directed left side, with curved apex (Fig. 2g, h). **Ootheca:** Dark yellow to creamy in colour, oval-shaped in dorsal view, dorsoventrally flattened. Rows of egg chambers that are parallel to the top and bottom of the egg, casing is visible from outside (Kolnegari and Vafaei 2018).

**Distribution.** Centre and north-east of Iran, Markazi province (Arak) (Kolnegari and Vafaei 2018), eastern Turkey (Yılmaz and Sevgili 2023), (Fig. 6: purple points).

We record this species for the first time from Khorasan Razavi, Mashhad, Iran.

**Conservation.** This species is widely distributed with an Extent of Occurrence (EOO) of about 290.000 km<sup>2</sup> in an apparently very fragmented number of locations (3) but

this number is probably underestimating the real number of locations. With no data on population trends over time, low anthropogenic presence and impacts in its known localities, this species can be addressed as Least Concern. Further research is however encouraged to collect more data and information on its real distribution and threats.

**Remarks.** The two paratypes of *H. brevipugilis* we were able to study and compare with our own material were collected at the same locality and on the same date as the holotype, so we are confident that they represent the same taxon. The original description of this species (Kolnegari 2018) was based on a very small number of specimens and on qualitatively variable morphological characters which were found to be present also in other species. A new species diagnosis is therefore proposed above, based on male genitalia here described for the first time.

The taxonomic status of *Holaptilon yagmur* underwent re-evaluation after determining its phylogenetic position within the genus. Our molecular genetic investigation revealed that the conventional reliance on external morphological traits for differentiating *H. yagmur* from other conspecifics within the genus lacked effectiveness in achieving precise species identification. Through comprehensive analysis of two mitochondrial (COI, 16S rDNA) and two nuclear DNA markers (H3, IDH), our molecular data showed that *H. yagmur* and *H. brevipugilis* are genetically indistinguishable or very closely related (Fig. 4). Consequently, *H. yagmur* should be considered synonymous with *H. brevipugilis*.

#### 4.6. *Holaptilon iranicum* Mirzaee and Sadeghi sp. nov.

<https://zoobank.org/0B8C3EF8-470C-4168-A12D-A4068A679F55>

Figure 9b, c

**Material examined.** Holotype: 1♂, pinned, with genitalia in a separate micro-vial, Arjan, Fars, Iran, 29.569N, 51.947E, 2100 m, 5/2021, leg. Mirzaee (SDEI). — Paratypes: 2♀, pinned, 1♀, 1 nymph, ethanol, Dasht Arjan, Fars, Iran, 29.569N, 51.947E, 2100 m, 5/2020, 5/2021, leg. Mirzaee (SDEI); 2♂, ethanol, Fasa, Fars, Iran, 29.176N, 53.380E, 1150 m, 7/2019, leg. Mirzaee (ZMPC); 1♀, ethanol, Sahlak, Fars, Iran, 29.176N, 53.380E, 1150 m, 7/2019, 2020, leg. Mirzaee (ZMPC); 1♂, 1 nymph, ethanol, Sahlak, Fars, Iran, 29.176N, 53.380E, 1150 m, 8/2021, 6/2022, leg. Mirzaee (ZMCBSU); 1♀, ethanol, Yasuj, Kohgiluyeh and Boyer-Ahmad, Iran, 30.713N, 51.618E, 1839 m, 8/2019, leg. Mirzaee (ZMPC); 1♀, ethanol, Arjan, Fars, Iran, 29.569N, 51.947E, 2100 m, 4/2021, leg. Mirzaee (ZMCBSU).

**Diagnosis.** Short, finger-like **afa**, which is markedly narrowed towards the apex and often curved near it. **pba** anterior of **afa** markedly sclerotised, posterior edge of **vla** markedly truncated (Fig. 2c, d).

**Description.** Males of this species are bigger and more robust than the males of the other species, but smaller

and more delicate in appearance than females. Males and females apterous, head and body dorsally pinkish in the individuals of Arjan districts, with small dark and black spots mostly in the middle of body parts; being entirely black ventrally in the individuals from Fasa and Sahlak districts, with small dark and black spots mostly in the middle of body parts. **Head:** Wider than high, two times wider than pronotum (Fig. 10c–e). **Pronotum:** Pentagonal shaped pronotum with rounded margin at the base, almost flat, compact. **Meso- and metanotum:** roof-shaped and finely keeled (Fig. 11d–f). **Forelegs:** Femora broad, dorsal edge lamellar, two times longer than wide, armed with 10–12 anteroventral spines with second one longer than the others; four discoidal spines with the first one shorter, the third one longer than the others, the second one is a bit smaller than the third one, the fourth is short but longer than the first one; four posteroventral spines, with the first one slightly longer than the other three spines, the first two spines are close to each other but the third and fourth more distant; anterior genicular lobe and posterior genicular lobe with a spine; foretibia armed with 10 anteroventral spines, elongating distally, and 12 posteroventral spines, also elongating distally. 1/2 part of all the spines on fore femora are black from top part and the base pale; the first three tarsomeres black, the others white (Fig. 12b). **Abdomen:** Entirely blackened in ventral view in both sexes of the individuals of Sahlak and Fasa districts, but the ventral side of the individuals from Arjan and Yasuj is light brown; slender but half as wide in male compared to female, the tergites weakly keeled in midline; supra-anal plate transverse, triangular; cerci with eight readily recognizable cercomeres, covered by long setae, last cercomere longer, but narrower than any of the others; subgenital plate much longer than wide. **Male genitalia:** Ventral phallomere oval, moderately wide. **afa** short, finger-like, markedly narrowed towards apex and often curved near it, strongly sclerotised, **pba** anterior of **afa** markedly sclerotised. Posterior edge of **vla** markedly truncated. Sclerite **L4B** curved, of complex shape, widened distally. Apical process **paa** long, directed left side, with blackened curved apex. (Fig. 2c, d). **Ootheca:** The ootheca was deformed. From the lateral view, it is convex and it has a yellow colour. The anterior end of the ootheca is smaller than the rest of it. Rows of egg chambers are parallel to the top and bottom of the egg casing (Fig. 13b).

**Measurements (in mm).** Body length: ♂ 12.5–15.0, ♀ 17.0–18.0; Head width: ♂ 3.0, ♀ 3.8–4.0; Head height: ♂ 1.5–2.2, ♀ 1.8–2.2; Pronotum length: ♂ 2.8–3.4, ♀ 3.5–3.6; Pronotum width: ♂ 2.5–3.5, ♀ 3.0–3.2, Forecoxa length: ♂ 3.0–3.6, ♀ 3.4–4.0, Forefemora length: ♂ 4.0–4.6, ♀ 4.0–4.3; Forefemora width: ♂ 2.0, ♀ 2.0.

**Distribution.** Southern Iran, Fars, and Kohgiluyeh and Boyer-Ahmad provinces (Arjan, Fasa, Sahlak, Darab, Dalkhan, Yasuj) (Fig. 6: yellow points).

**Habitat.** High in the mountains, surrounded by an abundance of rocks and vegetation, with a constant supply of water provided by winter snowfall (Fig. 7b).

**Conservation.** This species seems rather localised with an Extent of Occurrence (EOO) of about 1500 km<sup>2</sup> in a small number of locations (6), but presumably underestimated. With no data on population trends over time, and despite its natural habitat with low anthropogenic presence and impacts, this species might be addressed as Endangered, but further studies are needed to elucidate its threat status.

**Etymology.** The specific name “*iranicum*” refers to the country of origin, Iran.

#### 4.7. *Holaptilon khozestani* Mirzaee and Battiston sp. nov.

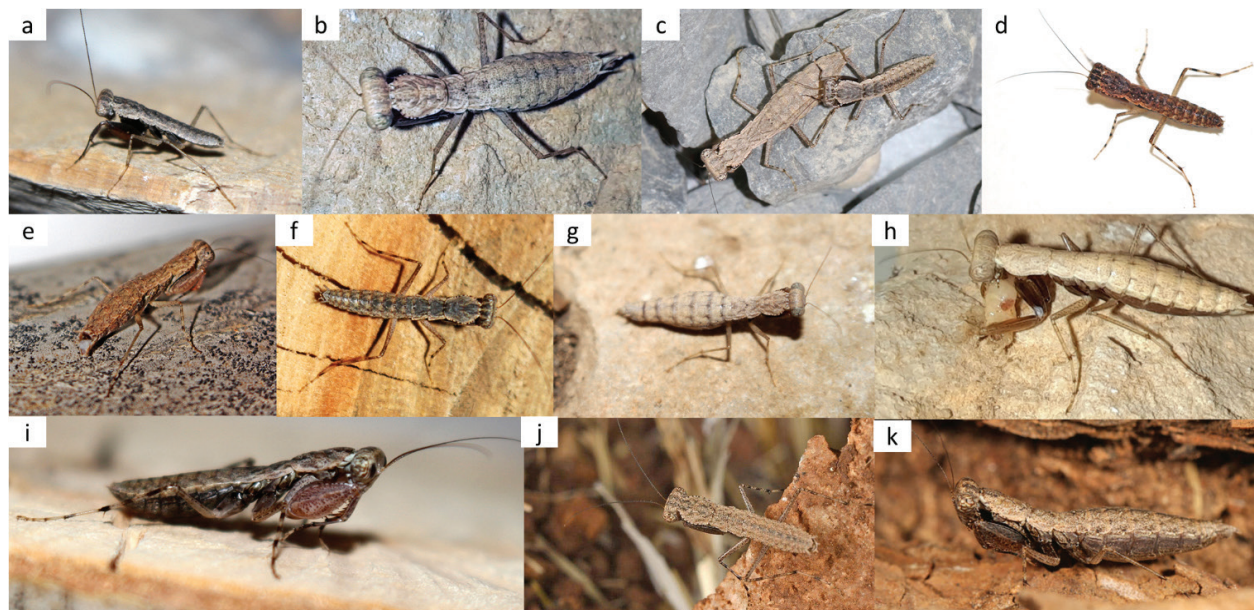
<https://zoobank.org/23CF3E3A-9B65-42DF-A278-3DC033304BD7>

Figure 9e, f

**Material examined.** Holotype: 1♂, ethanol, with genitalia in a separate micro-vial, Mal Agha, Khozestan, Iran, 31.607N, 49.998E, 1230 m, 7/2021, leg. Mirzaee (SDEI). — Paratypes: 3♀, ethanol, Dehdez, Khozestan, Iran, 31.733N, 50.222E, 1160 m, 6,7,8/2021, leg. Mirzaee (SDEI); 1♀, ethanol, Bagh Malek, Khozestan, Iran, 31.519N, 49.482E, 868 m, 7/2021, leg. Kiani (SDEI); 2 nymphs, ethanol, Mal Agha, Khozestan, Iran, 31.607N, 49.998E, 1230 m, 7/2021, leg. Mirzaee (SDEI); 4♂, 3♀ ethanol, Dehdez, Khozestan, Iran, 31.733N, 50.222E, 1160 m, 6,7,8/2021, leg. Mirzaee and Bakhshi (ZMPC); 1♀, ethanol, Bagh Malek, Khozestan, Iran, 31.519N, 49.482E, 868 m, 7/2021, leg. Kiani (ZMPC); 2♂, 5 nymphs, ethanol, Mal Agha, Khozestan, Iran, 31.607N, 49.998E, 1230 m, 7/2021, leg. Mirzaee and Bakhshi (ZMPC).

**Diagnosis.** Short, finger-like **afa**, **pba** anterior of the **afa** less sclerotised and truncation of the posterior edge of the **vla** (Fig. 2i, j).

**Description.** Males are way smaller and more delicate in appearance than females. Male and female apterous, body sandy brown in dorsal view, with some black spots mostly in the middle of body parts. **Head:** Wider than high, wider than pronotum (Fig. 10m–p). **Pronotum:** Almost flat, compact, wider than high in both sexes. **Meso- and metanotum:** roof-shaped and well keeled (Fig. 11m–p). **Forelegs:** Femora broad, dorsal edge lamellar, longer than wide, armed with 10–12 anteroventral spines in both males and females, with second one longer than the others; 4 discoidal spines with the first one shorter, the third one much longer than the others, the second one is a bit smaller than the third one; 4 posteroventral spines, with almost all of them having the same size, the first two spines are close to each other but the third and fourth have a bit more distance between them; anterior genicular lobe and posterior genicular lobe with a spine; foretibia armed with 9–10 anteroventral spines in both sexes, elongating distally, and 11–14 posteroventral spines in both sexes, also elongating distally (Fig. 12d). **Abdomen:** Slender but half as wide in male compared to female, the tergites keeled in midline; supra anal plate transverse, triangular;



**Figure 9.** Genus *Holaptilon* life habitus: **a** *H. abduallahii* **sp. nov.**, paratype male from Soroo, Busheher province (29.569N, 51.947E). **b** *H. abduallahii* **sp. nov.**, paratype female from Kangan, Busheher province (27.843N, 52.064 E). **c** *H. brevipugilis* male and female from Arak (34.128N, 50.07E) (photo credit: Mahmood Kolnegari). **d** *H. iranicum* **sp. nov.**, holotype male from Arjan, Fars province (29.569N, 51.947E). **e** *H. iranicum* **sp. nov.**, paratype female from Arjan, Fars province (29.569N, 51.947E). **f** *H. khozestani* **sp. nov.**, holotype male from Malagha, Khozestan province (31.607N, 49.998E). **g** *H. khozestani* **sp. nov.**, paratype female from Dehdez, Khozestan province (31.733N, 50.222E). **h** *H. tadovaniensis* **sp. nov.**, paratype female from Tadovan, Fars (28.853N, 53.326E). **i** *H. tadovaniensis* **sp. nov.**, holotype male from Tadovan, Fars (28.853N, 53.326E). **j** *H. pusillulum* male from Jerusalem, Israel (28.853N, 53.326E) (photo credit: More Yosef Avi). **k** *H. pusillulum* female from Jerusalem, Israel (31.737N, 35.077E) (photo credit: Chaym Turak).

cerci with nine readily recognizable cercomeres, covered by long setae; last cercomere longer and narrower than the others; subgenital plate much longer than wide. **Male genitalia:** Ventral phallomere oval, moderately wide. **Afa** short, finger-like, curved at the apex, **pba** anterior of the **afa** less sclerotised, the posterior edge of the **vla** truncated. Apical process **paa** long, directed right side, with curved apex (Fig. 2i, j). **Ootheca:** Creamy to yellow colour, with elliptical form in the dorsal view. It has a prominent dorsal point where the egg-case laying ended on the posterior end. The anterior end of the ootheca is smaller than the rest of it. Rows of egg chambers are parallel (Fig. 13c–e).

**Measurements (in mm).** Body length: ♂ 13–14, ♀ 18–20; Head width: ♂ 3.0–3.3; ♀ 4.0–4.1; Head height: ♂ 1.6, ♀ 2.0–2.2; Pronotum length: ♂ 3.3–3.5, ♀ 3.7–3.9; Pronotum width: ♂ 2.5–2.7, ♀ 3.0–3.2; Forecoxa length: ♂ 2.8–3.4, ♀ 3.6–4.0; Forefemora length: ♂ 3.5–4.2, ♀ 4.2–4.6; Forefemora width: ♂ 1.7–2.0, ♀ 2.2.

**Distribution.** South-west of Iran, Dehdez, Khozestan province (Fig. 6: blue points).

**Habitat.** High in the mountains, surrounded by an abundance of rocks and vegetation, with a permanent river (Fig. 7c).

**Conservation.** This species seems very localised with an Extent of Occurrence (EOO) of about 800 km<sup>2</sup> in a small number of locations (3). With no data on popula-

tion trends over time, despite its natural habitat with low anthropogenic presence and impacts, this species might be addressed as Endangered. Further studies are needed to clarify its threat status.

**Etymology.** The specific name “*khozestani*” refers to Khozestan province where the new species was found.

#### 4.8. *Holaptilon tadovaniensis* Mirzaee and Sadeghi **sp. nov.**

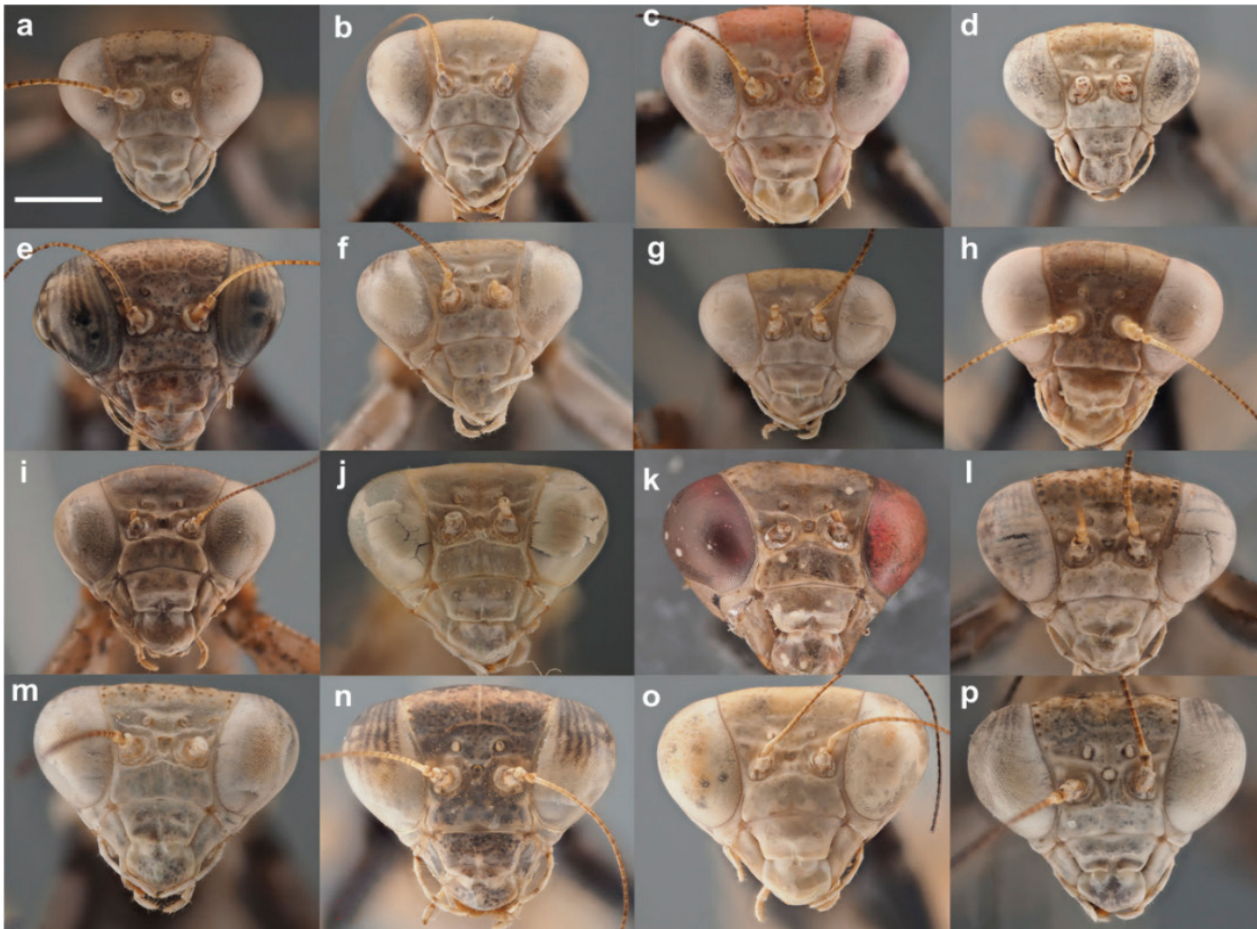
<https://zoobank.org/C310433E-CE49-454B-92BE-A3A1C-5C9A7EA>

Figure 9g, h

**Material examined.** Holotype: 1♂, ethanol, Tadovan, Fars, Iran, 28.853N, 53.326E, 1050 m, 7/2018, leg. Mirzaee (SDEI). — Paratypes: 1♂, 1♀, 2 nymphs, ethanol, Tadovan, Fars, Iran, 28.853N, 53.326E, 1050 m, 7/2018, leg. Mirzaee (ZMPC).

**Diagnosis.** Males of this species can be distinguished by short, finger-like **afa**, which is curved, and not narrowed towards apex, **pba** anterior of **afa** almost wholly sclerotised, the posterior edge of **vla** oblique and truncated, but the truncation is not as clear cut as in *H. iranicum* **sp. nov.**

**Description.** Males are much smaller and more delicate in appearance than females. Male and female apterous,



**Figure 10.** Heads of different *Holaptilon* species: **a** male (Kangan), **b** female (Kangan) *H. abdullahii* sp. nov.; **c** female (Arjan), **d** male (Arjan), **e** female (Sahlak), **f** female (Yasuj) *H. iranicum* sp. nov.; **g** male (Tadovan), **h** female (Tadovan) *H. tadovaniensis* sp. nov.; **i** female (Arak), **j** male (Mashhad), **k** female (Arak), **l** male (Arak) *H. brevipugilis*; **m** male (Dehdez), **n** male (Malagha), **o** male (Dehdez), **p** female (Dehdez) *H. khozestani* sp. nov.; scale bar: 1 mm.

body sandy brown in dorsal view, with some black spots mostly in the middle of body parts, and entirely blackened in ventral view (Fig. 2e, f). **Head:** Wider than high, slightly wider than pronotum (Fig. 10f–h). **Pronotum:** Almost flat, compact, wider than high in both sexes. **Meso- and metanotum:** roof-shaped and keeled in the midline (Fig. 11g, h). **Forelegs:** Femora broad, dorsal edge lamellar, longer than wide, armed with 12 anteroventral spines in both males and females, with second longer than the others; 4 discoidal spines with the first shorter, the third much longer than the others, the second is a bit smaller than the third; 4 posteroventral spines, with almost all of them of the same size, the first two spines are close to each other but the third and fourth have a bit more distance between them; anterior genicular lobe and posterior genicular lobe with a spine; foretibia armed with 9–11 anteroventral spines in both sexes, elongating distally, and 12–13 posteroventral spines in both sexes, also elongating distally (Fig. 12b). **Abdomen:** Slender but half as wide in male compared to female, the tergites keeled in midline, the ventral view completely black for both sexes; supra anal plate transverse, triangular; cerci with eight readily recognizable cercomeres, covered by long setae; last cercomere longer and narrower than the others; subgenital plate much longer than wide. **Male**

**genitalia:** Ventral phallomere oval, moderately wide. **afa** short, finger-like, curved, not narrowed towards apex, **pba** anteriad of **afa** almost wholly sclerotised; posterior edge of **vla** oblique, the “truncation” not as clear-cut as in *H. iranicum* sp. nov. Apical process **paa** long, directed left side, with curved apex (Fig. 2e, f). **Ootheca:** Unknown.

**Measurements (in mm).** Body length: ♂ 13.0, ♀ 17.0; Head width: ♂ 3.2, ♀ 3.4; Head height: ♂ 1.5, ♀ 1.8; Pronotum length: ♂ 3.0, ♀ 3.0; Pronotum width: ♂ 2.5, ♀ 2.5; Forecoxa length: ♂ 3.0, ♀ 3.3; Forefemora length: ♂ 3.5, ♀ 3.5; Forefemora width: ♂ 1.8, ♀ 1.8.

**Distribution.** South of Iran, Tadovan, Fars province (Fig. 6: orange point).

**Habitats.** High in the mountains, surrounded by an abundance of rocks and vegetation, with a permanent river (Fig. 7d).

**Conservation.** This species is known from a single locality. With no further data on distribution and population trends over time, this species can be addressed as Data Deficient.

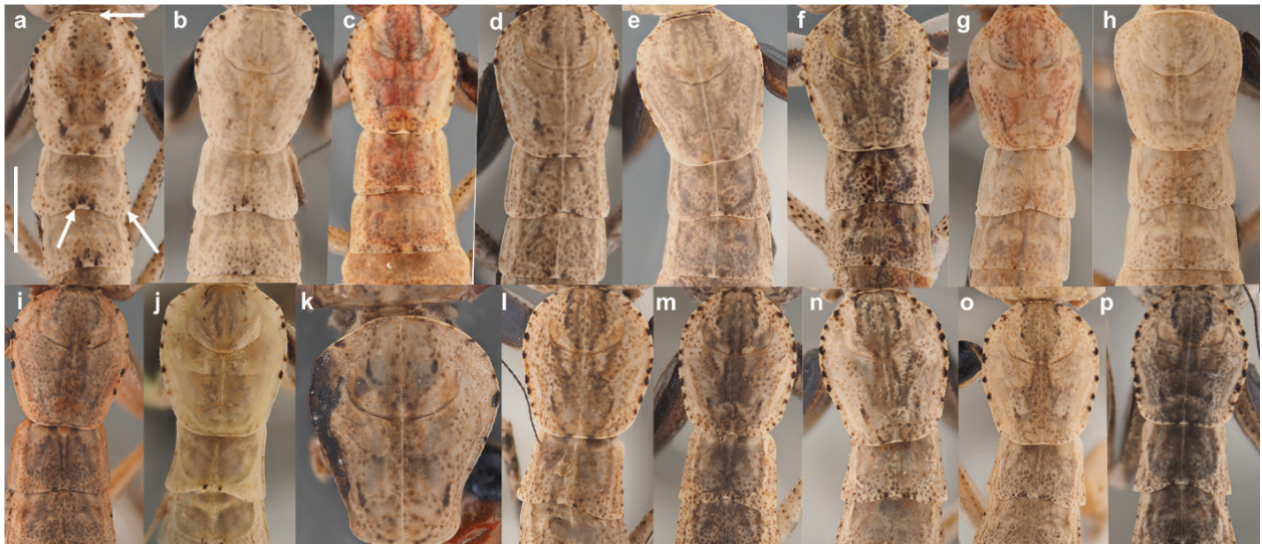


**Figure 11.** Posterior view of the thoraxes of different *Holaptilon* species: **a** male (Kangan) **b** female (Kangan) *H. abdullahii* **sp. nov.**; **c** female (Arjan), **d** male (Arjan), **e** female (Sahlak), **f** female (Yasuj) *H. iranicum* **sp. nov.**; **g** male (Tadovan), **h** female (Tadovan) *H. tadovaniensis* **sp. nov.**; **i** female (Arak), **j** male (Mashhad), **k** female (Arak), **l** male (Arak) *H. brevipugilis*; **m** male (Dehdez), **n** male (Malagha), **o** male (Dehdez), **p** female (Dehdez) *H. khozestani* **sp. nov.**; scale bar: 2 mm; white arrows indicate the characters that were used in the previous studies as diagnostic characters.

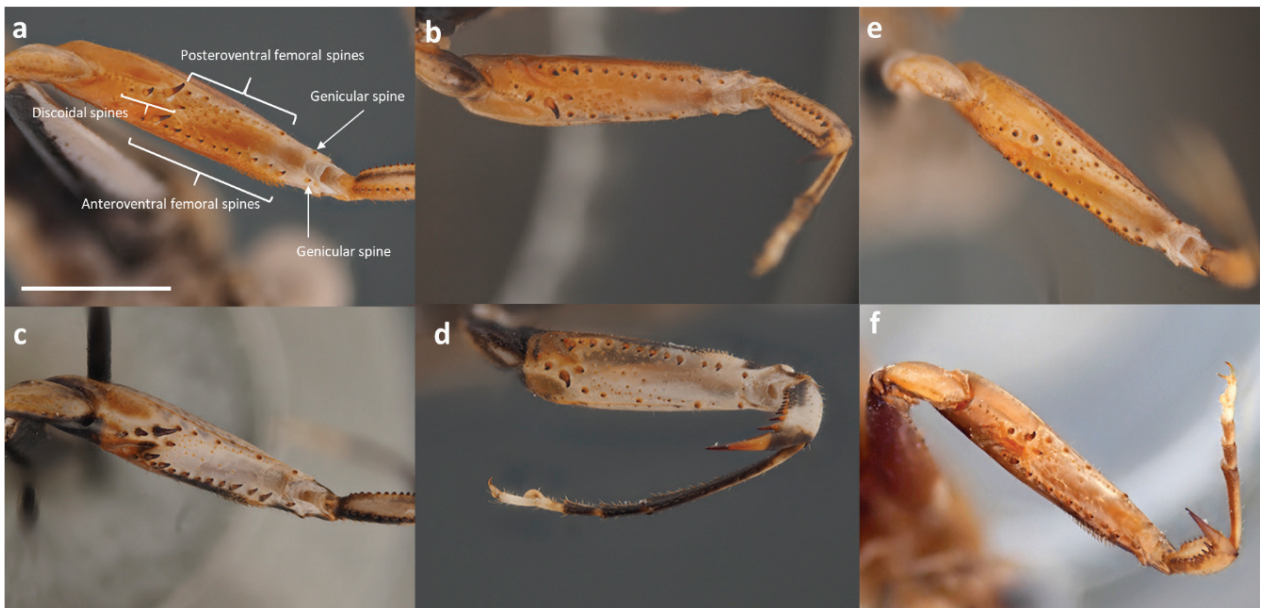


**Figure 12.** Different types of spines of the foreleg of different *Holaptilon* species: **a** female *H. iranicum* **sp. nov.**; **b** female *H. tadovaniensis* **sp. nov.**; **c** male *H. brevipugilis*; **d** male *H. khozestani* **sp. nov.**; **e** male *H. abdullahii* **sp. nov.**; **f** female *H. pusillum*; scale bar: 2 mm.

**Etymology.** The specific name “*tadovaniensis*” refers to the locality where the new species was found.

## 5. Life history and ecology

### 5.1. Field observations

*Holaptilon* individuals were observed in 16 districts of five provinces of Iran during different years by the first

author (2015–2022). The oothecae were found deposited under stones of different sizes. Oothecae were small, yellowish, with a spongy texture, delicate, and without apex (Fig. 13). Size range was 5–8 mm; larger oothecae contained eight eggs, the smaller ones five to six. Females tended to lay their oothecae in small, already existing holes in stones.

Nymph emergence observations of *H. abdullahii* **sp. nov.** were made from mid-March onwards, adults were observed from the end of May to the end of July (males) and the end of August (females). Nymph emergence observations of *H. iranicum* **sp. nov.** were made from mid-

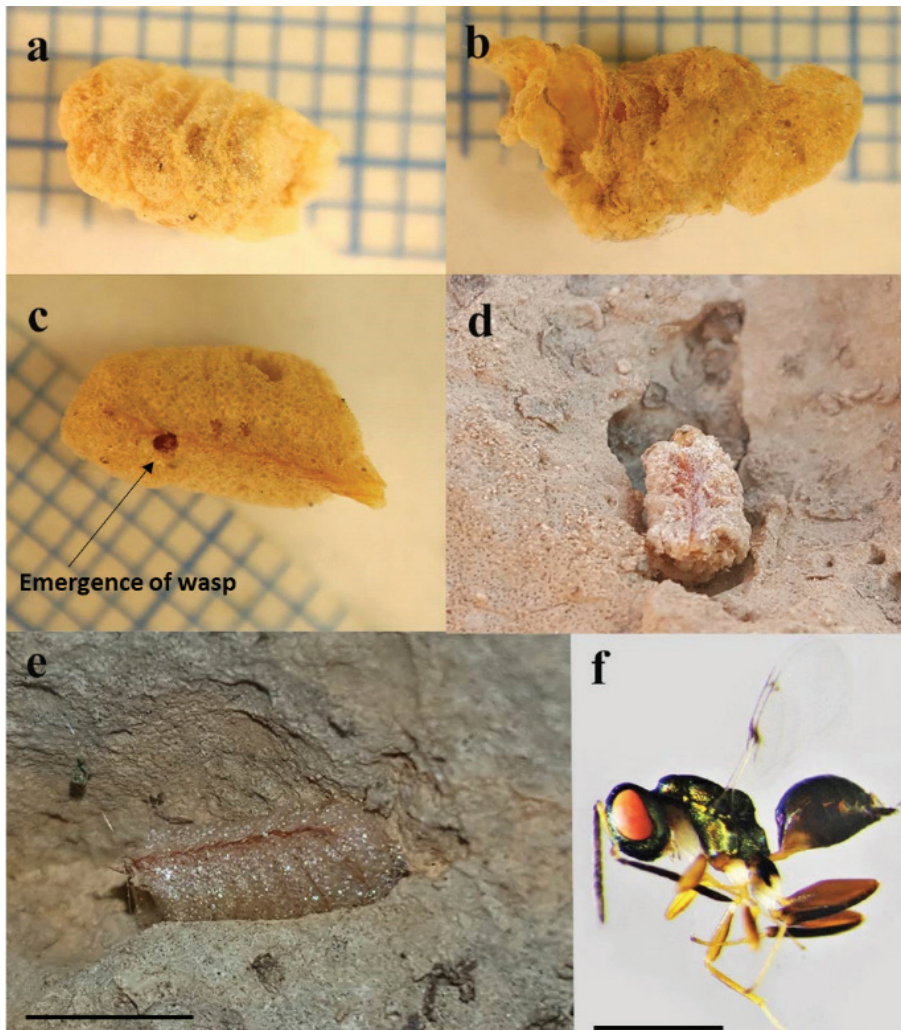


**Figure 13.** Ootheca of different *Holaptilon* species: **a** *H. abduallahii* **sp. nov.**; **b** *H. iranicum* **sp. nov.**; **c–e** *H. khozestani* **sp. nov.**; **f** *Palachia pulchra*, parasitoid wasp which parasitizes *Holaptilon* ootheca; scale bar for the oothecae: 3 mm, for the wasp: 0.5 mm.

May, adults were observed from the first week of August to the end of September (males) and the end of October (females). Nymph emergence observations for *H. khozestani* **sp. nov.** were made from the first week of July, adults were observed from the end of August to the end of October (males) and the end of November (females). Nymph emergence observations for *H. tadovaniensis* **sp. nov.** were made from mid-February onwards, adults were observed from the end of July to the end of August (males) and mid-September (females).

Adult males ( $N \geq 15$ ) were running between or on rocks during the hottest time of the day in August. They were observed actively running between stones during the day and on the ground at night. Seven of the 15 observed males were approaching females from the backside and suddenly jumped on their backs. Females ( $N \geq 21$ ) were mostly found under stones. All known habitats had natural water sources like permanent rivers or springs.

*H. abduallahii* **sp. nov.** females were exclusively observed beneath stones, while the behaviour of males differed. Some males ( $N = 6$ ) were discovered while overturning stones, others were observed running on the ground towards light sources at night ( $N = 1$ ). Additionally, some males were seen running between or on stones during midday in Tombak ( $N = 2$ ), Kangan ( $N = 2$ ), and Soroo ( $N = 1$ ). The elevational range of the locations

where specimens of this species were found varied from 10 to 637 m above sea level (asl).

One female of *H. iranicum* **sp. nov.** from Yasuj was found under *Astragalus* sp., whereas both females and males from Sahlak were observed among grasses. In Arjan and Fasa, males and females of this species were discovered under stones. Elevation ranged from 1000 to 1800 m asl.

*H. khozestani* **sp. nov.**, females and males were primarily observed under stones ( $N = 8$ ), but three males were found running on the ground. The elevation ranged from 800 to 2000 m asl.

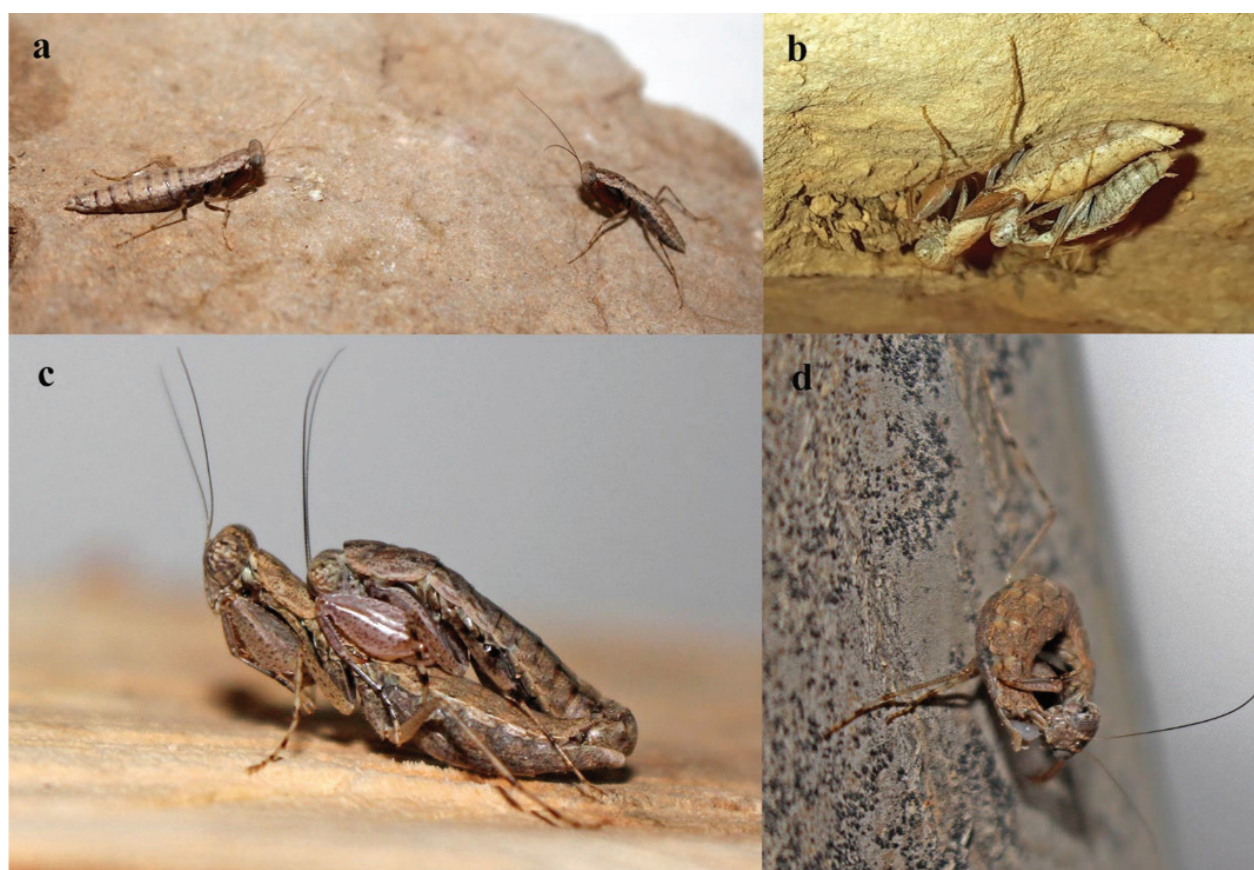
Regarding *H. tadovaniensis* **sp. nov.**, one female and two males of this species were discovered under stones ( $N = 3$ ). The elevation was approximately 1000 m asl.

## 5.2. Laboratory observations

The oothecae of different species were collected from their natural habitats. They hatched eight to nine weeks after being collected. Ootheca sizes, incubation duration, number of eggs per ootheca, and number of hatched nymphs are given in Table 2. Two oothecae of *H. khozestani* were parasitised by *Palachia pulchra* Bouček, 1969 (Fig. 13) (Mirzaee et al. 2021). No mantid nymph

**Table 2.** Field collected oothecae under lab condition.

Species	Width (mm)	Length (mm)	Incubation duration (days)	No. of eggs	No. of hatched nymphs	No. of emerged wasps
<i>H. abdullahii</i>	3.1	8.1	58	12	5	0
<i>H. abdullahii</i>	3	5.7	57	8	5	0
<i>H. abdullahii</i>	3.9	3.9	60	4	2	0
<i>H. iranicum</i>	2.1	7.1	62	8	5	0
<i>H. iranicum</i>	3.0	8.0	66	10	0	0
<i>H. khozestani</i>	2.8	7.0	59	8	0	12
<i>H. khozestani</i>	2.8	4.8	58	4	3	0
<i>H. khozestani</i>	3.4	5.4	59	7	0	10
<i>H. khozestani</i>	2.8	7.8	65	8	3	0
<i>H. khozestani</i>	2.6	5.6	65	6	2	0
Mean	2.95	5.90	60.90	7.40	3.1	NA
SD	0.57	2.97	1.41	5.66	2.12	NA

**Figure 14.** Reproduction in *Holaptilon*: **a** male and female in front orientation; **b** mating failure of *H. iranicum* **sp. nov.** male trying to mate with *H. khozestani* **sp. nov.** female; **c** successful mating of *H. khozestani* **sp. nov.**; **d** spermatophore feeding of *H. khozestani* **sp. nov.**

emerged from these two oothecae; 12 and 9 parasitoids emerged instead, respectively. Each male individual moulted five times and each female six times to reach adult stage. The observed male courtship display was the same as observed by Kolnegari (2020) for *H. brevipugilis*, and it consisted of bending the abdomen up and downward, moving the antennae fast, sometimes with trembling boxing forelegs alternately, and jumping on the back of the female. The trembling boxing forelegs were mostly observed when males were facing females (90% of males). Most of the males tried to approach females

from the back (11 males). Six males also ran towards females and jumped on them from the front (Fig. 14). Seven males approached females laterally. All 24 males were successful in the mating process. Mating duration was four to seven hours. No cannibalism was observed. Spermatophore feeding behaviours were observed for all 31 females (Fig. 14d).

Three males of *H. iranicum* from Arjan district were introduced to three females of *H. khozestani*. Two of these males tried to escape from the females, and they avoided facing them. One male approached the respective

female and jumped on its back but was unable to successfully mate (Fig. 14b). After three hours attempting, the male's reproductive organ still failed to connect with the female's reproductive organ, resulting in an unsuccessful attempt. As a result, the male was removed from the female. Two males of *H. abdullahii* were introduced to two females of *H. iranicum*, both of which attempted to escape from the females.

## 6. Discussion

### 6.1. General remarks on the genus *Holaptilon*

Beier (1964) described the type species *H. pusillum* and mentioned that the femora of this genus have four very short external spines. However, our study revealed that *H. abdullahii* **sp. nov.** possesses five short external spines on the femora. Additionally, Beier (1964) noted that the anterior tibiae of this genus have 13 short external spines, while our research indicated that the number of spines on the anterior tibiae is variable, ranging from 9 to 13. Furthermore, Beier (1964) mentioned that this genus belongs to the Gonypetini tribe, which is primarily distributed in the Oriental region. However, our study demonstrated that not all genera within this tribe, such as *Holaptilon*, are restricted to the Oriental region, but are also distributed in the Palearctic region. In addition, the genus *Elaea* Stål, 1877, also belonging to Gonypetini, is distributed from Africa to SW Asia.

### 6.2. Morphological species delimitation

In previous studies on *Holaptilon*, a rather limited number of 2–5 specimens were utilised to characterise new species in this genus. Our study represents the first comprehensive revision of the genus, counting on the examination of 87 specimens. Based on the examination of this material, we show that all the characters previously used as diagnostic characters at the species level were actually within the range of intraspecific variation, not allowing species delimitation.

In fact, a notable amount of variability was observed across different traits. Historically, male genitalia attributes served as traditional tools for describing and classifying mantid species. However, given the pronounced variability observed, this approach has not been effectively employed for certain species within the genus *Holaptilon*, such as *H. pusillum*, *H. brevipugilis*, and *H. yagmur*.

Although some aspects of male genital structures, specifically the curvature or sclerotisation of phallosome processes like **afa**, **pba**, or **vla**, might at times offer a secondary qualitative differentiation, the prevailing variability inherent in both male and female genital

structures renders this trait inconclusive for species characterisation. The variation in male genitalia within the genus *Holaptilon* could be attributed to a combination of factors, including limited ranges without overlap and hence missing sexual selection among species; in turn, high species range overlap of closely related species should be associated with remarkable sexual selection. Investigating the interplay between these factors and their effects on male genitalia diversity would provide valuable insights into the complex mechanisms driving the observed variation in this character complex. With regard to colouration, our study revealed that the spots and colouration of the inner view of the fore-femora of *Holaptilon* species varies among specimens of the same species and is thus not suitable for distinguishing species (Fig. S5). Variability in the foreleg colouration and spot patterns was also observed in other Mantodea, such as *Anasigerpes* Giglio-Tos, 1915 (Roy, 1965). A comparable level of intraspecific variability is evident in other characters, such as the degree of concavity of the posterior margin of the meso- and metanotum or the number of posteroventral spines of the foretibiae (Fig. 12; Suppl. Material File 2: Table S2). Similarly, the shape of the thorax, supra-anal plate, and the numbers of posteroventral spines of the foretibiae, which previously were used to distinguish the three so far known *Holaptilon* species (Yılmaz and Sevgili 2023; Figs 11, 12, 15; Table S2) are also variable. Such a level of variation could be related to the relatively young clade status of the group. The limited time for divergence, high genetic diversity, incomplete reproductive isolation, adaptive potential, and the possibility of rapid speciation, all may contribute to the wide range of phenotypic traits and characteristics observed among the species in this genus.

Consequently, describing *Holaptilon* species based on a limited number of specimens and relying solely on external morphology to define and distinguish the species, as hitherto conducted, is unreliable and does not deliver adequate characters for a morphometric separation of species in this genus. In order to surmount these taxonomic challenges, we adopted alternative approaches, aiming to identify distinct morphological characters and understand morphological variability which can potentially offer valuable insights into the evolutionary narrative of *Holaptilon* species.

For this purpose, hypervolume analyses were employed for the evaluation of the morphological data regarding measurements of different body parts, ratios of the body parts with respect to each other, and also counting different spine types on the raptorial legs. The outcomes of our ecological, phylogenetic, and morphological analyses revealed low overlap (i.e., distinctiveness) between *H. tadovaniensis* **sp. nov.** and *H. iranicum* **sp. nov.**, and high overlap between *H. khozestani* **sp. nov.** and *H. abdullahii* **sp. nov.** followed by *H. brevipugilis* and *H. khozestani* **sp. nov.** These results could be explained by their ecological similarity, while the groups recovered in fact inhabit similar habitats—specifically their tendency to inhabit the spaces beneath stones in mountainous regions with a permanent water source

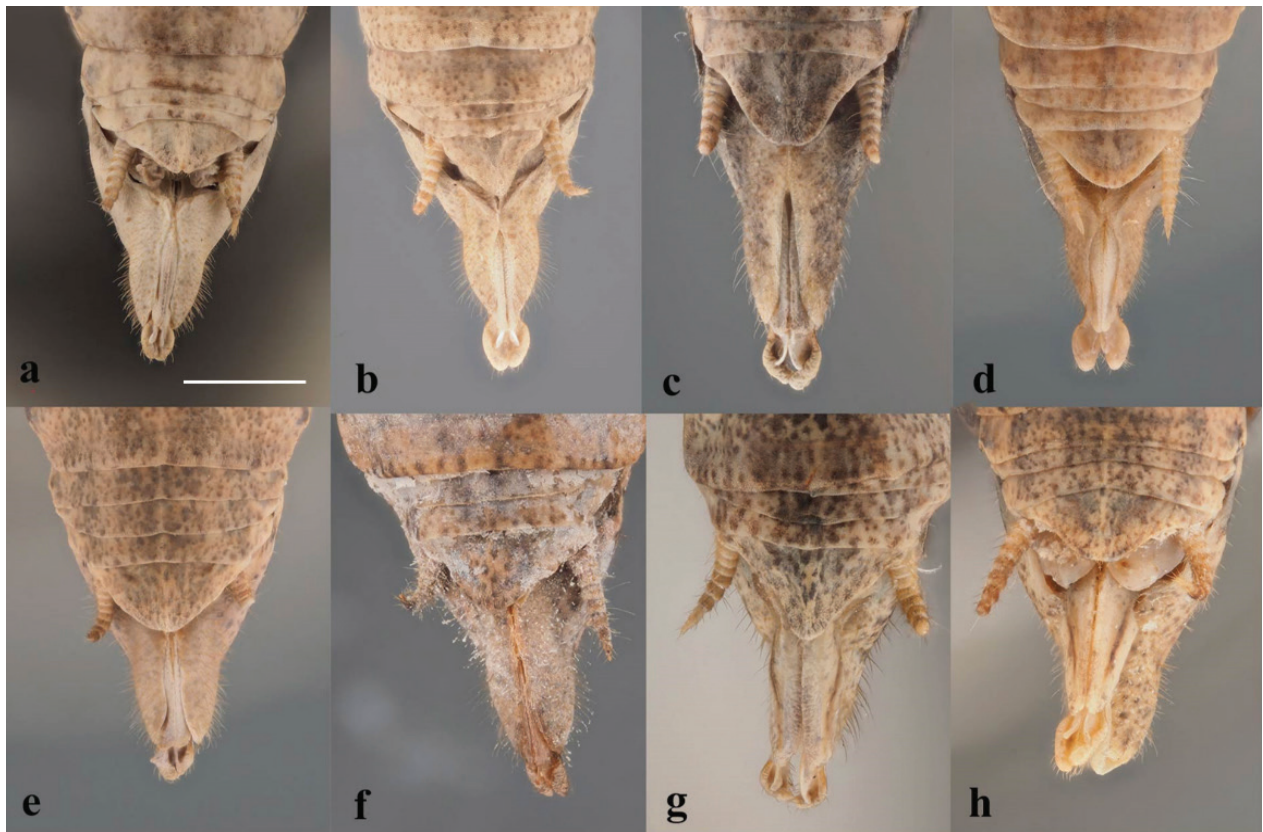


**Figure 15.** Posterior view of supra-anal plate of the females of two *Holaptilon* species that shows the variation in this character, **a–d** *H. iranicum* **sp. nov.**; **e–h** *H. khozestani* **sp. nov.**; scale bar: 2 mm.

(Fig. 7). This, in combination with the variation in external morphology among individual and their closely intertwined phylogenetic relationships, potentially contribute to the patterns recovered (Tables S6, S7, Figs S3, S4).

### 6.3. Molecular phylogenetics

Most of the nodes of the phylogenetic trees had high support (1/100) (Fig. 4). The ASAP algorithm of nuDNA supported our hypothesis on the existence of 6 species, whereas the bPTP and the mPTP algorithm suggested an additional species split within *H. khozestani* **sp. nov.** However, the ASAP, bPTP, and mPTP algorithms of combined genes and mtDNA genes alone far overestimated the number of species; the detected species numbers were considerably higher for all combined genes and mtDNA, than the morphologically distinguishable ones and the ones distinguished by nuDNA. These high species number detections could also be an artifact due to the small sample size available from many populations: Most of the clades are represented by few individuals (several times only one), making a concise delimitation of species by an algorithm questionable. Adding more individuals might solve this problem, a difficult task in such a rare and difficult-to-spot genus as *Holaptilon*. Nevertheless, a general pattern exists among all outputs: All algorithms suggest that *H. iranicum* **sp. nov.**, *H. khozestani* **sp. nov.**, and *H. brevipugilis* are possibly split

further into cryptic species, which form distinct clades within the tree separated by long branches due to high genetic distances. Therefore, their existence or at least separate evolutionary units within these three species (and thus a wider hidden variability and biodiversity in this mantid genus) cannot be excluded. This hypothesis needs to be tested more thoroughly using a larger number of samples.

### 6.4. Divergence time and biogeography

The biogeographic analysis provided intriguing insights into the evolution and historical range dynamics of the genus *Holaptilon*, shedding light on its potential origin and the evolutionary pathways of its species. Unfortunately, it was not feasible to incorporate genera closely related to *Holaptilon* as outgroups in the RASP analysis due to a lack of available information and challenges associated with obtaining specimens for conducting the relevant analyses. Nonetheless, the results suggest a compelling narrative of range shifts and vicariant events that have shaped the distribution of *Holaptilon* over millions of years.

The biogeographical reconstruction proposed that the genus *Holaptilon* likely originated in the southern parts of Zagros mountains (south-western Iran, area A) dating back at least 6 million years (Mya). This is also supported by the fact that four of the six known species occur in the

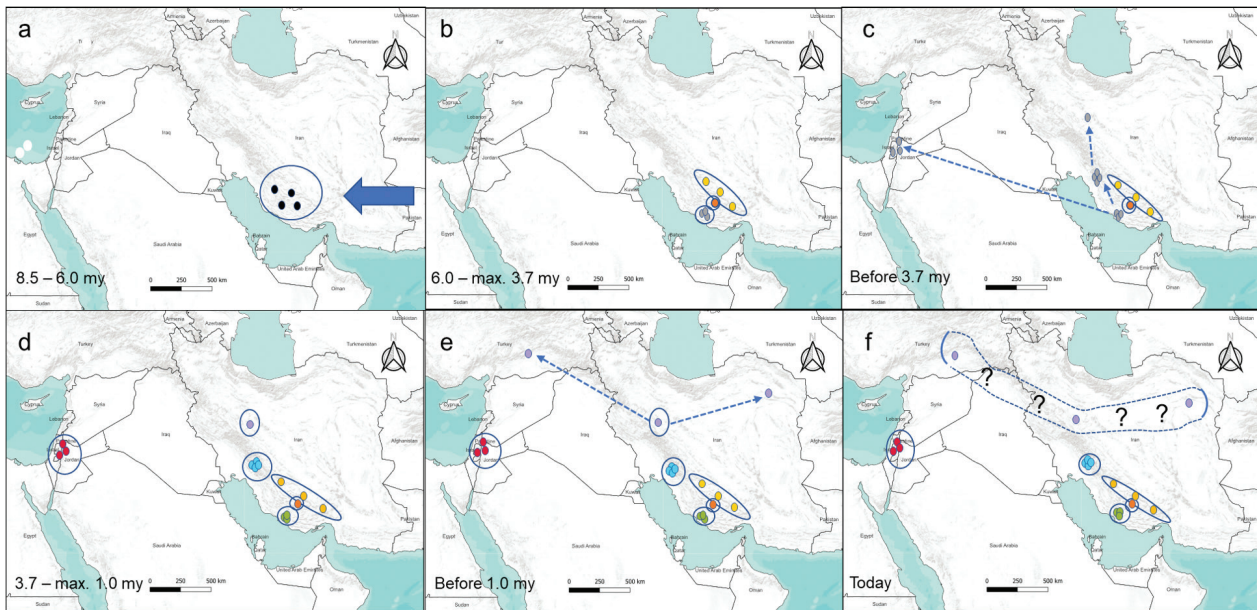


**Figure 16.** Historical biogeography of *Holaptilon* with possible range expansions and retractions.

Zagros Mountains forest steppe ecoregion (Dinerstein et al. 2017); in addition, *H. abdullahii* is restricted to the desertic coastal region south of these mountains, i.e. the western edge of the South Iran Nubo-Sindian desert and semi-desert. The most recent common ancestor of all extant *Holaptilon* species should have reached the southern Zagros region immigrating from the east (where most extant relatives of the genus are found) in the late Miocene, dating back as far as 8.5 Myr, as indicated by the 95% highest posterior density (HPD) interval (Fig. 16a). This ancient origin is underlining the deep evolutionary history of the genus. An important turning point in the history of *Holaptilon* apparently coincided with the Messinian Salinity Crisis (5.96–5.33 Mya) (Krijgsman et al. 1999). This period of environmental upheaval and increased aridity in the greater Mediterranean region (Hsü et al. 1977) likely triggered the fragmentation and isolation of populations within southern Iran, resulting in the basal split into three lineages of which two evolved into the species *H. iranicum* and *H. tadovaniensis*, the third into the other four species (Fig. 16b).

While *H. iranicum* and *H. tadovaniensis* most likely remained close to their centre of origin (i.e., area A) throughout time without major range dynamics, it must have been the third basal *Holaptilon* lineage that expanded prior to 3.7 Mya out of the southern foothills of Zagros to north-western Iran (area B) and further westwards to Palestine (area E) (Fig. 16c). This large range must have been successively fragmented a little later into four parts, in each of which one *Holaptilon* species evolved (Fig. 16d). This range fragmentation most likely took place in a relatively short time window (i.e., at 3.7–3.4 Mya), maybe triggered by the climate cooling known in the late Pliocene, although that seems to have happened somewhat later (i.e., 3.2 Mya) (Thunell 1979; Bertoldi et al. 1989). This period of isolation likely played a pivotal role in enhancing genetic divergence and promoting speciation, thereby reinforcing the ge-

netic distinctiveness of populations occupying discrete regions.

At latest 1.0 Myr ago, another important range expansion has to be postulated for the by then already existing species *H. brevipugilis* from north-western Iran (area B), in western direction to south-eastern Turkey (area C) and in eastern direction to north-eastern Iran (area D), followed by (at least temporal) range fragmentation and vicariance about 1.0 Myr ago (Fig. 16e). These range dynamics might have been triggered by the cyclic fluctuations of the Pleistocene, possibly in particular by the Mid-Pleistocene Transition (1.2–0.8 Mya) (Berends et al. 2021). However, the time elapsed since this initial vicariance event was apparently not sufficient for further speciation. However, due to the difficulties in spotting these mantids in the field, it is unknown whether the extant distribution of *H. brevipugilis* is mostly continuous from south-eastern Turkey to north-eastern Iran or highly fragmented, maybe in just three core areas (Fig. 16f).

## 6.5. Life history, ecology and conservation

The species belonging to this genus are restricted to geographically small areas, making them particularly susceptible to the risk of extinction due to the combined effects of climate change and human activities. However, they also exhibit some traits that make them excellent bioindicators, similar to other praying mantids. This means that changes in their population and behaviour can provide valuable insights into the overall health and ecological balance of their habitats (Battiston et al. 2020).

According to this research, all members of this genus appear to be univoltine, with only one generation per year. This is almost the same for most temperate mantid species (Hogue and Powell 1980).

The size, shape, and colour of mantid oothecae can be influenced by different biotic and abiotic factors, such as temperature, food availability, humidity, genetics, the presence of males (Robert 1937; Breland and Dobson 1947; Hurd et al. 1995), natural enemies that parasitise or prey on their eggs such as chalcidoids of the families Eupelmidae, and Torymidae (Mirzaee et al. 2021a), clerid beetles such as *Trichodes* (Coleoptera: Cleridae), dermestid beetles such as *Attagenus*, *Dermestes*, *Orphinus*, and *Thaumaglossa* (Kershaw 1910; Hawkeswood 2003; Mirzaee et al. 2022a), as well as other arthropods (Mirzaee et al. 2021b). These factors not only have the potential to influence the structure of oothecae, but also the population dynamics of mantids in the wild. The oothecae of *Holaptilon* species in this study were also affected by these factors, such as parasitisation by the parasitoids *Palachia pulchra* and deformation, for which we assumed some of the factors mentioned above (Table 2, Fig. 13).

Males in a variety of insects transfer sperm to females via an externally attached spermatophore, which the females then remove and consume. Males in most Mantodea genera transfer sperm to females via internally placed spermatophores. In *Holaptilon* species, the male inserts the spermatophore with its genitalia into the female's genital chamber, from which it is expelled (while still attached) and consumed by the female. (Fig. 14d). This behaviour might be due to an adaptation of *Holaptilon* species to the rather harsh environmental conditions they live in, where every source of nutrition is extremely valuable. It also might be the reason why cannibalism is not observed in *Holaptilon*, as females receive some sort of "gift" when mating with males. Holwell (2007) documented this behaviour for the first time in four species of *Ciulfina* Giglio-Tos, 1915. This behaviour was documented among other females of Mantodea species, e.g., *Hierodula tenuidentata* (Mirzaee et al. 2022b), and seems to be a well-known phenomenon in Mantodea (Bischoff et al. 2001). Two species in this genus, *H. iranicum* and *H. tadovaniensis*, coexist in the same habitats, sharing remarkably similar morphology, including reproductive structures, but exhibit distinct genetic patterns (Fig. 4). The evolutionary divergence of these cryptic species requires in-depth exploration of their behavioural patterns. Notably, sexual selection in cannibalistic mantids can be a potent evolutionary driver, and the presence of courtship behaviours and the occurrence of unsuccessful mating attempts in laboratory conditions suggest that further research is needed to investigate this perspective.

The conservation status of the different species of *Holaptilon* is variable and a full knowledge on the real distribution, presence localities, population trends and threats for each single species is still lacking and further researches in this way are encouraged. However, in this preliminary evaluation, four species were assessed as Endangered (*abdullahii*, *iranicum*, *khazestani*, *pusillulum*), one as Data Deficient (*tadovaniensis*) and one as Least Concern (*brevipugilis*). On a general and preliminary level, these species seem to need urgent conservation efforts to improve their status.

## 7. Conclusion

Our comprehensive investigation of the genus *Holaptilon* has yielded significant advancements in our understanding of the taxonomy, phylogeny, biogeography, and ecology of these mantids. By employing a combination of different analytical methods, we successfully addressed the challenges associated with traditional species delimitation and classification in this genus. First, the examination of a larger and diverse set of specimens allowed us to unravel the intraspecific variation in morphological characters that were previously used for species identification. It became evident that these characters are not reliable for distinguishing species, as they exhibit significant variability among individuals. This discovery prompted us to question the validity of previously described species and emphasised the need for a more rigorous taxonomic approach. Second, this molecular phylogenetic analysis yielded high-support trees which shed light on the genetic relationships among *Holaptilon* species. Our results reinforce the usefulness of incorporating genetic data into taxonomic studies for a comprehensive understanding of species diversity. Thirdly, the combined utilisation of external morphological, morphometric, and hypervolume analyses facilitated the identification of suitable morphological characters for species identification and enabled us to understand variation within and among species with unclear morphological boundaries. This alternative approach helped us to overcome limitations of traditional morphological classifications, which often relied on unreliable external characteristics in this genus. Furthermore, the integration of ecological and life history aspects added a deeper understanding of these mantids' adaptation and interaction within their environment, unravelling the univoltine life cycle of each species and their reproductive pattern.

Therefore, using all these methods resulted in describing four new *Holaptilon* species (*H. abdullahii* sp. nov., *H. khazestani* sp. nov., *H. iranicum* sp. nov., *H. tadovaniensis* sp. nov.) and synonymisation of *H. yagmur* with *H. brevipugilis*. However, it also showed the need for further studies with additional data to study the possible existence of further cryptic species within *H. khazestani*, *H. iranicum* and *H. brevipugilis*, all of which showed high genetic intraspecific differentiation (Fig. 4). The knowledge gained from combining all these analyses in this study can serve as a valuable foundation for more informed conservation efforts and future research in this poorly known group of insects, aiding in their protection and further enriching our understanding of their ecological roles and evolutionary history.

## 8. Conflicts of Interest

The authors declare no conflict of interest.

## 9. Acknowledgments

The authors express their gratitude to Ahmad Katbeh-Bader (University of Jordan) for providing the specimen of *H. pusillum* from Jordan and to Evgeny Shcherbakov (Lomonosov Moscow State University, Russia) for his careful reviews and valuable comments. We also extend our gratitude to Hossein Abdollahi, Yaser Bakhshi, and Mohammad Javad Ghasempour for their help during fieldwork, as well as Mahdi Ghafarnia for collecting and supplying valuable specimens from Mashhad, Khorasan Razavi Province. Furthermore, we are thankful to Amir Weinstein, Dany Simon, and Benny Shalmon (Steinhardt Museum of Natural History, Tel Aviv, Israel) for providing two males, three females and one nymph from the type locality of *H. pusillum*, Mahmood Kolnegari for providing two females and one male of *H. brevipugilis* from Arak, Iran, and to Kaan Yılmaz and Hassan Sevgili for providing one leg of *H. yagmur* for molecular analyses. We also thank Mahmood Kolnegari, Chaym Turak and More Yosef Avi for providing photos of live adults of *H. brevipugilis* and *H. pusillum*, respectively.

## 10. References

- Abu-Dannoun O, Katbeh-Bader A (2007) Mantodea of Jordan. *Zootaxa* 1617(1): 43–56. <https://doi.org/10.11646/zootaxa.1617.1.2>
- Allen LA, Barry KL, Holwell GI (2012) Mate location and antennal morphology in the praying mantid, *Hierodula majuscula*. *Austral Entomology* 51: 133–140. <https://doi.org/10.1111/j.1440-6055.2011.00843.x>
- Anisimova M, Gil M, Dufayard JF, Dessimoz C, Gascuel O (2011) Survey of branch support methods demonstrates accuracy, power, and robustness of fast likelihood-based approximation schemes. *Systematic Biology* 60(5): 685–699. <https://doi.org/10.1093/sysbio/syr041>
- Barry KL, Holwell GI, Herberstein ME (2008) Female praying mantids use sexual cannibalism as a foraging strategy to increase fecundity. *Behavioural Ecology* 19: 710–715. <https://doi.org/10.1093/beheco/arm156>
- Battiston R, Amerini R, Di Pietro W, Guariento LA, Bolognin L, Moretto E (2020) A new alien mantis in Italy: is the Indochina mantis *Hierodula patellifera* chasing the train for Europe? *Biodiversity Data Journal* 8: e50779. <https://doi.org/10.3897/BDJ.8.e50779>
- Battiston R, Galliani C (2011) On the life-cycle of *Ameles spallanzania* (Rossi, 1792) (Insecta, Mantodea). *Natural History Sciences* 152(1): 25–35. <https://sisn.pagepress.org/index.php/nhs/article/download/nhs.2011.25/47/95>
- Beier M (1964) Ein neues Mantiden-Genus aus Israel. *Israel Journal of Zoology* 13: 184–186.
- Berends CJ, Köhler P, Lourens LJ, van de Wal RSW (2021) On the cause of the mid-Pleistocene transition. *Reviews of Geophysics* 59: e2020RG000727. <https://doi.org/10.1029/2020RG000727>
- Bertoldi R, Rio D, Thunell R (1989) Pliocene-Pleistocene vegetational and climatic evolution of the south-central Mediterranean. *Palaeogeography, Palaeoclimatology, Palaeoecology* 72: 263–275. [https://doi.org/10.1016/0031-0182\(89\)90146-6](https://doi.org/10.1016/0031-0182(89)90146-6)
- Birkhead TR, Lee KE, Young P (1988) Sexual cannibalism in the praying mantis *Hierodula membranacea*. *Behaviour* 106: 112–118. <https://doi.org/10.2307/4534701>
- Bischoff I, Bischoff R, Heßler C, Meyer M (2001) *Praxis Ratgeber: Mantiden – Faszinierende Lauerjäger*. Edition Chimaera, Frankfurt. 191 pp.
- Blonder B, Lamanna C, Violle C, Enquist BJ (2014) The n-dimensional hypervolume. *Global Ecology and Biogeography* 23(5): 595–609. <https://doi.org/10.1111/geb.12146>
- Blonder B (2016) Pushing past boundaries for trait hypervolumes: A Response to Carmona et al. *Trends in Ecology & Evolution* 31(9): 665–667. <https://doi.org/10.1016/j.tree.2016.07.001>
- Blonder B (2018) Hypervolume concepts in niche- and trait-based ecology. *Ecography* 41(9): 1441–1455. <https://doi.org/10.1111/ecog.03187>
- Bouckaert R, Vaughan TG, Barido-Sottani J, Duchêne S, Fourment M, Gavryushkina A, et al. (2019) BEAST 2.5: An advanced software platform for Bayesian evolutionary analysis. *PLoS Computational Biology* 15(4): e1006650. <https://doi.org/10.1371/journal.pcbi.1006650>
- Bordenstein SR, O'Hara FP, Werren JH (2001) *Wolbachia*-induced incompatibility precedes other hybrid incompatibilities in *Nasonia*. *Nature* 409: 707–710. <https://doi.org/10.1038/35055543>
- Brannoch SK, Svenson GJ (2016) Leveraging female genitalic characters for generic and species delimitation in *Nilomantis* Werner, 1907 and *Ilomantis* Giglio-Tos, 1915 (Mantodea, Nilomantinae). *Insect Systematics & Evolution*, 47(3): 209–244. <https://doi.org/10.1163/1876312X-47032141>
- Brannoch SK, Wieland F, Rivera J, Klass K-D, Bethoux O, Svenson GJ (2017) Manual of praying mantis morphology, nomenclature and practices (Insect, Mantodea). *ZooKeys* 696: 1–100. <https://doi.org/10.3897/zookeys.696.12542>
- Breland OP (1941) *Podagrion mantis* Ashmead and other parasites of praying mantid egg cases (Hym.: Chalcidoidea; Dipt.: Chloropidae). *Annals of the Entomological Society of America* 34: 99–113. <https://doi.org/10.1093/aesa/34.1.99>
- Darriba D, Taboada GL, Doallo R, Posada D (2012) jModelTest 2: more models, new heuristics and parallel computing. *Nature Methods* 9(8): 772. <https://doi.org/10.1038/nmeth.2109>
- Dinerstein E, Olson D, Joshi A, Vynne C, Burgess ND, Wikramanayake E, Hahn N, Palminteri S, Hedao P, Noss R, Hansen M (2017) An ecoregion-based approach to protecting half the terrestrial realm. *BioScience* 67(6): 534–545. <https://doi.org/10.1093/biosci/bix014>
- Guindon S, Gascuel O (2003) A simple, fast, and accurate algorithm to estimate large phylogenies by maximum likelihood. *Systematic Biology* 52(5): 696–704. <https://doi.org/10.1080/10635150390235520>
- Handal E, Al Wahsh A, Ehrmann R, Amr Z, Battiston R, Qumsiyeh M (2018) Mantids (Dictyoptera: Mantodea) from the Palestinian Territories with an updated list. *Articulata* 33: 91–105.
- Hawkeswood TJ (2003) Notes on the biology and food items of three Australian Dermestidae (Coleoptera). *Calodema* 1: 1–4.
- Hoang DT, Chernomor O, Von Haeseler A, Minh BQ, Vinh LS (2018) UFBoot2: improving the ultrafast bootstrap approximation. *Molecular Biology and Evolution* 35(2): 518–522. <https://doi.org/10.1093/molbev/msx281>
- Hogue CL, Powell JA (1980) *California Insects*. University of California Press, Berkeley, 400 pp.
- Hsü KJ, Montadert L, Bernoulli D, Cita MB, Erickson A, Garrison RE, Kidd RB, Mèlières F, Müller C, Wright R (1977) History of the Mediterranean salinity crisis. *Nature* 267(5610): 399–403. <https://doi.org/10.1038/267399a0>
- Hurd LE, Eisenberg RM, Moran MD, Rooney TP, Gangloff WJ, Case VM (1995) Time, temperature, and food as determinants of population persistence in the temperate mantid *Tenodera sinensis* (Mantodea: Mantidae). *Environmental Entomology* 24: 348–353. <https://doi.org/10.1093/ee/24.2.348>

- Hurvich CM, Tsai CL (1989) Regression and time series model selection in small samples. *Biometrika* 76(2): 297–307. <https://doi.org/10.1093/biomet/76.2.297>
- Kapli P, Lutteropp S, Zhang J, Kobert K, Pavlidis P, Stamatakis A, Flouri T (2017) Multi-rate Poisson tree processes for single-locus species delimitation under maximum likelihood and Markov chain Monte Carlo. *Bioinformatics* 33: 1630–1638. <https://doi.org/10.1093/bioinformatics/btx025>
- Kershaw JC (1910) The formation of the ootheca of a Chinese mantis, *Hierodula saussuri*. *Psyche* 17: 136–141. <https://doi.org/10.1155/1910/78374>
- Kolnegari M, Vafaie R (2018) The first Persian boxer mantid: a new species of *Holaptilon* Beier, 1964 from Haftad-gholeh protected area, Iran (Mantodea, Mantidae). *Entomological Research Journal* 10: 150–158.
- Krijgsman W, Hilgen FJ, Raffi I, Sierro FJ, Wilson DS (1999) Chronology, causes and progression of the Messinian salinity crisis. *Nature* 400(6745): 652–655.
- Leong TM (2009) Oviposition and hatching in the praying mantis, *Hierodula patellifera* (Serville) in Singapore (Mantodea: Mantidae: Paramantinae). *Nature in Singapore*, 2: 55–61.
- Mirzaee Z, Lotfalizadeh H, Sadeghi S (2021a) Chalcidoid parasitoids (Hymenoptera: Torymidae and Eupelmidae) of mantids (Mantodea) oothecae in Iran. *Phytoparasitica* 50(2): 487–499. <https://doi.org/10.1007/s12600-021-00965-1>
- Mirzaee Z, Ebrahimi M, Sadeghi S, Battiston R, Hajian M (2021b) Mantid ootheca (Insecta: Mantodea: *Hierodula*) or a home for many arthropods? *Iranian Journal of Science and Technology Transaction A* 45: 1925–1931. <https://doi.org/10.1007/s40995-021-01184-3>
- Mirzaee Z, Sadeghi S, Hava J, Battiston R, Ruzzier E (2022a) New observations of Coleoptera associated with Mantodea ootheca and an overview of the previous records. *Bulletin of Insectology* 75(2): 223–230. <http://www.bulletinofinsectology.org/pdfarticles/vol75-2022-223-230mirzaee.pdf>
- Mirzaee Z, Sadeghi S, Battiston R (2022b) Biology and life cycle of the praying mantid *Hierodula tenuidentata* Saussure, 1869 (Insecta: Mantodea). *Iranian Journal of Science and Technology Transaction A*, Science, 46: 1163–1169. <https://doi.org/10.1007/s40995-022-01325-2>
- Narita S, Nomura M, Kato Y, Fukatsu T (2006) Genetic structure of sibling butterfly species affected by *Wolbachia* infection sweep: evolutionary and biogeographical implications. *Molecular Ecology* 15: 1095–1108. <https://doi.org/10.1111/j.1365-294X.2006.02857.x>
- Nguyen LT, Schmidt HA, Von Haeseler A, Minh BQ (2015) IQ-TREE: a fast and effective stochastic algorithm for estimating maximum-likelihood phylogenies. *Molecular Biology and Evolution* 32(1): 268–274. <https://doi.org/10.1093/molbev/msu300>
- Posada D (2008) jModelTest: phylogenetic model averaging. *Molecular Biology and Evolution* 25(7): 1253–1256. <https://doi.org/10.1093/molbev/msn083>
- Puillandre N, Brouillet S, Achaz G (2021) ASAP: assemble species by automatic partitioning. *Molecular Ecology Resources* 21(2): 609–620. <https://doi.org/10.1111/1755-0998.13281>
- Rambaut A, Drummond AJ, Xie D, Baele G, Suchard MA (2018) Posterior Summarization in Bayesian Phylogenetics using Tracer 1.7. *Systematic Biology* 67(5): 901–904. <https://doi.org/10.1093/sysbio/syy032>
- Raut GA, Bhawane GP, Gaikwad SM (2014) Laboratory studies on the life history of *Hierodula ventralis* Giglio-Tos, 1912 (Mantodea: Mantidae). *Journal of Entomology and Zoology Studies* 2(6): 147–152. <https://www.entomoljournal.com/archives/2014/vol2issue6/PartC/49.pdf>
- Ritter S, Michalski SG, Settele J, Wiemers M, Fric ZF, Sielezniew M, Sasic M, Rozier Y, Durka A (2013) *Wolbachia* infections mimic cryptic speciation in two parasitic butterfly species, *Phengaris telei* and *P. nausithous* (Lepidoptera: Lycaenidae). *PLoS ONE* 8(11): e78107. <https://doi.org/10.1371/journal.pone.0078107>
- Robert RA (1937) Biology of the bordered mantid, *Stagmomantis limbata* Hahn (Orthoptera, Mantidae). *Annals of the Entomological Society of America* 30: 97–109. <https://doi.org/10.1093/aesa/30.1.96>
- Rodriguez F, Oliver JL, Marín A, Medina JR (1990) The general stochastic model of nucleotide substitution. *Journal of Theoretical Biology* 142(4): 485–501. [https://doi.org/10.1016/S0022-5193\(05\)80104-3](https://doi.org/10.1016/S0022-5193(05)80104-3)
- Roy R (1965) Les Mantes de la Guinée forestière. *Bulletin de l'Institut Français d'Afrique Noire, Série A*, 27(2):577–613.
- Schwarz CJ, Roy R (2019) The systematics of Mantodea revisited: an updated classification incorporating multiple data sources (Insecta: Dictyoptera). *Annales de la Société Entomologique de France, New Series*, 55: 101–196. <https://doi.org/10.1080/00379271.2018.1556567>
- Thunell RC (1979) Climatic evolution of the Mediterranean Sea during the last 5.0 million years. *Sedimentary Geology* 23(1–4): 67–79. [https://doi.org/10.1016/0037-0738\(79\)90006-X](https://doi.org/10.1016/0037-0738(79)90006-X)
- Wendt M, Kulaneck D, Varga Z, Rákossy L, Schmitt T (2022) Pronounced mito-nuclear discordance and various *Wolbachia* infections in the water ringlet *Erebia pronoe* have resulted in a complex phylogeographic structure. *Scientific Reports* 12(1): 5175. <https://doi.org/10.1038/s41598-022-08885-8>
- Whitworth TL, Dawson RD, Magalon H, Baudry E (2007) DNA barcoding cannot reliably identify species of the blowfly genus *Protophthora* (Diptera: Calliphoridae). *Proceedings of the Royal Society B* 274: 1731–1739.
- Yilmaz K, Sevgili H (2023) The genus *Holaptilon* Beier, 1964: discussion on the poorly known boxer mantis genus, with a new species (Mantodea, Gonypetidae). *Zootaxa* 5231(4): 427–444. <https://doi.org/10.11646/zootaxa.5231.4.5>
- Yu Y, Blair C, He XJ (2020) RASP 4: Ancestral state reconstruction tool for multiple genes and characters. *Molecular Biology and Evolution* 37(2): 604–606. <https://doi.org/10.1093/molbev/msz257>
- Zheng C, Ye Z, Zhu X, Zhang H, Dong X, Chen P, Bu W (2020) Integrative taxonomy uncovers hidden species diversity in the rheophilic genus *Potamometra* (Hemiptera: Gerridae). *Zoologica Scripta* 49(2): 174–186. <https://doi.org/10.1111/zsc.12401>

## Supplementary Material 1

### Tables S1

**Authors:** Mirzaee Z, Battiston R, Ballarin F, Sadeghi S, Simões M, Wiemers M, Schmitt T (2024)

**Data type:** .xlsx

**Explanation notes:** **Table S1.** Occurrences and GenBank accession numbers.

**Copyright notice:** This dataset is made available under the Open Database License (<http://opendatacommons.org/licenses/odbl/1.0>). The Open Database License (ODbL) is a license agreement intended to allow users to freely share, modify, and use this Dataset while maintaining this same freedom for others, provided that the original source and author(s) are credited.

**Link:** <https://doi.org/10.3897/asp.82.e112834.suppl1>

## Supplementary Material 2

### Tables S2–S7

**Authors:** Mirzaee Z, Battiston R, Ballarin F, Sadeghi S, Simões M, Wiemers M, Schmitt T (2024)

**Data type:** .docx

**Explanation notes:** **Table S2.** Spines counted on both left and right front legs. — **Table S3.** Ratio of different body parts in relation to each other. — **Table S4.** Measurements of different parts of the body. — **Table S5.** List of primers used in amplifying and sequencing gene fragments, with the corresponding source and PCR conditions. — **Table S6.** Pairwise morphological comparison of the studied *Holaptilon* species based on n-dimensional hypervolumes 3PC. — **Table S7.** Pairwise morphological comparison of the studied *Holaptilon* species based on n-dimensional hypervolumes 4PC.

**Copyright notice:** This dataset is made available under the Open Database License (<http://opendatacommons.org/licenses/odbl/1.0>). The Open Database License (ODbL) is a license agreement intended to allow users to freely share, modify, and use this Dataset while maintaining this same freedom for others, provided that the original source and author(s) are credited.

**Link:** <https://doi.org/10.3897/asp.82.e112834.suppl2>

## Supplementary Material 3

### Figures S1–S5

**Authors:** Mirzaee Z, Battiston R, Ballarin F, Sadeghi S, Simões M, Wiemers M, Schmitt T (2024)

**Data type:** .docx

**Explanation notes:** **Figure S1.** Morphometrical ratios of PL/PW (Pronotum length/ Pronotum width); HW/HH (Head width/ Head height); LFH/LFW (Lower frons width/Lower frons height); FL/FW (Femur length/Femur width); MsL/MsW (Mesonotum width/Mesonotum length); MtL/MtW (Metanotum width/ Metanotum length), HW/PW (Head width/ Pronotum width); PL/HH (Pronotum length/Head height) of a) males and b) females of different *Holaptilon* species. — **Figure S2.** Morphometrical ratios of HL/HW (Head width/ Head height); and PL/PW (Pronotum length/ Pronotum width); in a) females and b) males of different *Holaptilon* species. — **Figure S3.** Estimated n-dimensional hypervolumes for the five species listed in the bottom left. — **Figure S4.** Estimated nine-dimensional hypervolumes for the five species listed in the bottom left. — **Figure S5.** Variability of colouration and spots on the forelegs of different individuals of *Holaptilon iranicum* sp. nov.

**Copyright notice:** This dataset is made available under the Open Database License (<http://opendatacommons.org/licenses/odbl/1.0>). The Open Database License (ODbL) is a license agreement intended to allow users to freely share, modify, and use this Dataset while maintaining this same freedom for others, provided that the original source and author(s) are credited.

**Link:** <https://doi.org/10.3897/asp.82.e112834.suppl3>